February 6, 1975

To the Graduate Council:

I am submitting herewith a dissertation written by Quentin Douglass Craft, entitled "Solvent Isotope Effects in the H_2O-D_2O-NaCl System: Enthalpies and Free Energies of Solution." I recommend that it be accepted in partial fulfillment of the requirements for the degree of Doctor of Philosophy, with a major in Chemistry.

W. Alexander Van Hook, Major Professor

We have read this dissertation
and recommend its acceptance:

Accepted for the Council:

Vice Chancellor
Graduate Studies and Research

SOLVENT ISOTOPE EFFECTS IN THE H_2O-D_2O-NaCl SYSTEM: ENTHALPIES AND FREE ENERGIES OF SOLUTION

A Dissertation

Presented for the

Doctor of Philosophy

Degree

The University of Tennessee

Quentin Douglass Craft

March 1975

ACKNOWLEDGMENT

The author would like to sincerely acknowledge the friendship, guidance, and encouragement given by Dr. W. Alexander Van Hook during the course of this work. Appreciation is also extended to the National Science Foundation for financial assistance during three years, and to the Tennessee Eastman Company for a one year fellowship.

Special thanks go to Rebecca Craft for her constant support and inspiration. The author wishes to thank Dr. Robert G. Gaunder. He is also indebted to Mrs. Joyce Wallace for the typing of this dissertation.

The author would like to dedicate this work to his parents.

1214562

ABSTRACT

The solvent isotope effects in sodium chloride solutions of normal (H_2O) and heavy (D_2O) water (especially at low concentration) were investigated. Freezing point depressions in normal and heavy water are reported from $\sim$ 0.01 to $\sim$ 2 m. A new value of the heat of fusion of D_2O (-1507 ± 3 cal $mole^{-1}$) was determined. Values of the partial molal enthalpies are derived from differential heats of solution of sodium chloride in both isotopic waters from 0.01 to 4 m and from 5 to 40°. The freezing point data are used to obtain osmotic coefficients at the freezing points of the solutions (H_2O and D_2O), and the enthalpy data allow calculation of the osmotic coefficient at temperatures up to 40°. The present data establish the sodium chloride-D_2O system as an isopiestic reference for future measurements on solutions using D_2O as solvent.

The isotope effect on the relative partial molal enthalpy of the sodium chloride and on the osmotic coefficient shows a $\sqrt{m}$ concentration dependence within experimental error.

TABLE OF CONTENTS

CHAPTER		PAGE
I.	INTRODUCTION	1
II.	EXPERIMENTAL	4
	A. Materials	4
	B. Freezing Points: Apparatus and Procedures	4
	1. Freezing point measurements	4
	2. Apparatus	5
	3. The temperature scale	7
	4. Determination of concentration	8
	5. Errors	10
	6. Isotopic analysis	11
	7. Experimental procedure	12
	C. Calorimetry: Apparatus and Procedures	13
	1. Calorimetric experiments	13
	2. Adiabatic calorimetry	14
	3. Isothermal calorimetry	20
III.	RESULTS	26
	A. Background	26
	B. Enthalpies	30
	1. H_2O data	30
	2. Fitting of $\overline{L}_{2H}$	33
	3. Calculation of $\overline{L}_{1H}$	37
	4. D_2O data and isotope effects	38
	5. Fit of $\overline{L}_{2H}-\Delta H_D^{df}$ to the Extended Debye-Hückel Equation	43

CHAPTER PAGE

6. Heats of dilution 45
7. Integral heats 50
8. Heat capacities 54
C. Osmotic Coefficient Data from the Measurement of Freezing Point Depressions 57
1. Thermodynamics 57
2. H_2O data 59
3. Fitting of ϕ_H (0°) from all freezing point data and discussion of errors 62
4. D_2O data 65
5. Heat of fusion of D_2O: The Intercept 67
6. Isotope effect on ϕ 69
7. The fitting of $\Delta\phi$ as a function of m 70
8. Calculation of $\Delta\phi$ at other temperatures 77
9. Comparisons with literature 78
10. Calculation of ΔG_2° 82
IV. DISCUSSION 84
A. Introduction 84
B. Heat of Fusion of D_2O 84
C. Reliability of the Data 85
1. H_2O data 85
2. Isotope effects 87
V. CONCLUSIONS 91
LIST OF REFERENCES 92
APPENDICES 97

APPENDICES PAGE

I. CALIBRATION DATA FOR THERMISTOR AND PLATINUM THERMOMETER 98

II. TABULAR SUMMARY OF ISOTOPE EFFECTS 101

III. ENTHALPY DATA FOR OTHER SALTS 105

VITA 107

LIST OF TABLES

TABLE		PAGE
I.	Error Analysis of Freezing Point Data	10
II.	Experimental Values of ΔH_H^{df} and $\bar{L}_{2H}$ for NaCl in H_2O	31
III.	Literature Values of $\bar{L}_{2H}$	34
IV.	Experimental Values of ΔH_D^{df} and $(\bar{L}_{2H}-\Delta H_D^{df})$	39
V.	Heats of Dilution (ΔH^{dil}) in H_2O and D_2O	47
VI.	Slopes of $\Delta\phi H_2$ with Respect to $\sqrt{m}$	49
VII.	Integral Heats of Solution (ΔH^I) of NaCl in H_2O and D_2O	52
VIII.	Values of ΔL_2^s for NaCl	53
IX.	Values of $\Delta\bar{C}_p^\circ$ ($\Delta\phi_c^\circ$) from ΔL_2^s	55
X.	Freezing Point Depressions in H_2O	60
XI.	Freezing Point Depressions for NaCl in D_2O	68
XII.	Isotope Effect on the Osmotic Coefficient at 3.82°C	71
XIII.	Fits of $\Delta\phi$ to Empirical Functions	73
XIV.	Fits of $\Delta\phi$ to Forms of the Extended Debye-Hückel Equation	76
XV.	Calibration of Thermistor	99
XVI.	Summary of Isotope Effects in H_2O-D_2O-NaCl System	101
XVII.	Heats of Dilution for KCl	105
XVIII.	Integral Heats of Solution and Isotope Effects for Other Salts	106

LIST OF FIGURES

FIGURE		PAGE
1.	Freezing Point Apparatus	6
2.	Adiabatic Calorimeter	15
3.	Temperature vs. Time Plot for Adiabatic Calorimeter . . .	18
4.	Isothermal Calorimeter Vessel	21
5.	Plot of $\overline{L}_{2H}$ as a Function of m	36
6.	Plot of $(\overline{L}_{2H}-\Delta H_D^{df})$ vs. $\sqrt{m}$	41
7.	Deviation Plot for All Freezing Point Data	63
8.	Fit of $\phi_H-\phi_D(\Delta\phi)$ at 3.82°	75
9.	Temperature Dependence of $\Delta\phi$	79
10.	Comparison (at 40°) of $\Delta\phi$ from Vapor Pressure (Circles) with $\Delta\phi$ from Present Work (Line).	80

CHAPTER I

INTRODUCTION

Water and its solutions have been of general scientific interest for many years. The voluminous literature has been recently reviewed by Franks.[1] Similarly aqueous solvent isotope effects have been of scientific concern since the discovery and isolation of heavy water (D_2O). Progress in the field has been reviewed by Arnett and McKelvey,[2] Friedman and Krishnan,[3] Bigeleisen, Lee, and Mandel,[4] and most recently by Jancso and Van Hook.[5] One of the major advantages of studies of isotope effects is that they allow for a modest perturbation of the system without causing a complete disappearance of the property of interest. Isotopic isomers are assumed to execute their motions on identical potential energy surfaces, at least within the range of validity of the Born-Oppenheimer approximation.[6,7] The interpretation of isotope effects is based on the well established conclusion that isotope effects are model sensitive properties of the system.[4,5,8] It follows that solvent isotope effects can be used as probes in the investigation of certain details of the potential energy surface describing the motion of solvent molecules, in other words the structure of the solution.

Several investigators have reported on the solvent isotope effect in aqueous solutions. The most extensive investigations have been those of Pupezin, Jakli, Jancso, and Van Hook[9] and Chan, Jakli, and Van Hook[10] who used vapor pressure measurements to determine isotope effects on solvent activities for a series of electrolyte solutes dissolved in H_2O

and D_2O between roughly 0 and 100°. Other work includes the e.m.f. measurements of Schrier and Schrier[11] and the isopiestic measurements of Kerwin.[12]

None of the previous studies have yielded precise isotope effects on the solvent activity at low salt concentration. Corresponding properties of the solute can be determined by a Gibbs-Duhem-Bjerrum integration, but a proper calculation requires knowledge of solvent properties to the infinite dilution limit. Previously,[9,10] the isotope effect on solvent activities was extrapolated to infinite dilution using values above 1 molal. Although it has been reasonably assumed[9,10] that the isotope effect on the solvent activity is a better behaved function than the solvent activity of either solvent, the extrapolation is still an important matter for concern from the practical as well as the theoretical viewpoint.

Robertson and LaMer[13] and Scatchard, Jones, and Prentiss[14] have demonstrated that freezing point measurements can yield solvent activities of high precision at low salt concentration. Values of the relative partial molal enthalpy of the solvent are needed to correct the solvent activities to a common temperature and to extend the data to higher temperatures.

It was in the context of the consideration detailed above that a program was initiated to calorimetrically determine relative partial molal enthalpies of H_2O and D_2O and to determine solvent activities by measuring freezing point depressions in H_2O and D_2O. Looking forward to future isopiestic measurements, we thought it advantageous to obtain high precision data for a single salt, NaCl (as opposed to less precise

measurements on a series of salts) and to use the improved data in a refinement of the theoretical interpretation of the solvent isotope effect.

CHAPTER II

EXPERIMENTAL

A. Materials

All normal water (H_2O) used in the measurements was doubly distilled. The second distillation was made from basic potassium permanganate solution using an all glass still. Reagent grade heavy water (D_2O) with a minimum isotopic purity of 99.8 mole percent (conductivity < 1.5×10^{-5} mhos·cm^{-3}) was obtained from Bio-Rad Laboratories. This was first used without further purification, but after each run the D_2O was reclaimed by distillation and reused. No differences were detected between any of the different D_2O samples. Isotopic analysis of the D_2O was carried out as described below (p. 11). Reagent grade NaCl (Fisher Scientific Company) recrystallized two times from doubly distilled water was used in all measurements. NaCl used to make standard solutions and used for calorimetric measurements was dried overnight at 180° prior to use. The reagent grade silver nitrate for the titrations (J. T. Baker Chemical Company) was used without further purification since it was not a primary standard.

B. Freezing Points: Apparatus and Procedures

1. Freezing Point Measurements

The equilibrium method first used by Richards[15] was employed for the measurement of the freezing point depressions. Our choice of this method was dictated in part by convenience but more directly from considerations concerning the measurement of the isotope effects. The

freezing point of a saline solution is a function of three variables: the concentration, solvent activity, and the isotopic analysis of the solvent. Of the three, the last is hardest to control since D_2O is hygroscopic. However, difficulties connected with isotopic dilution can be minimized by employing the same sample of solvent as both reference and unknown. Thus a sample of ice and water was placed in the apparatus, a thermal base line established, and only then was salt added. After equilibrium was attained, the new temperature was recorded and at the same time a sample was taken for concentration and isotopic analysis and the freezing point depression calculated.

2. Apparatus

A schematic diagram of the freezing point apparatus is shown in Figure 1. It consists of a medium sized Dewar ($\sim$ 300 cm^3) closely fitted with a teflon cap through which two stirrers and the necessary thermistor leads enter. One stirrer runs continuously while the second which consists of a simple wide loop was only used intermittently in order to prevent the formation of aggregates of ice.

The thermistor (Veco #32A1, 2000 nominal ohms at 25°, $(dR/dT)_{0°} \tilde{=}$ 300 ohms deg^{-1}) electrically composes one leg of a dc Wheatstone bridge which will be described in detail in the following section (p 14) (it was also used as part of our adiabatic calorimeter). The thermistor resistance was readily calculated from the measured bridge output (read with a Leeds and Northrup K-4 potentiometer) and the voltage of the mercury cell powering the bridge circuit which was checked independently for each run.

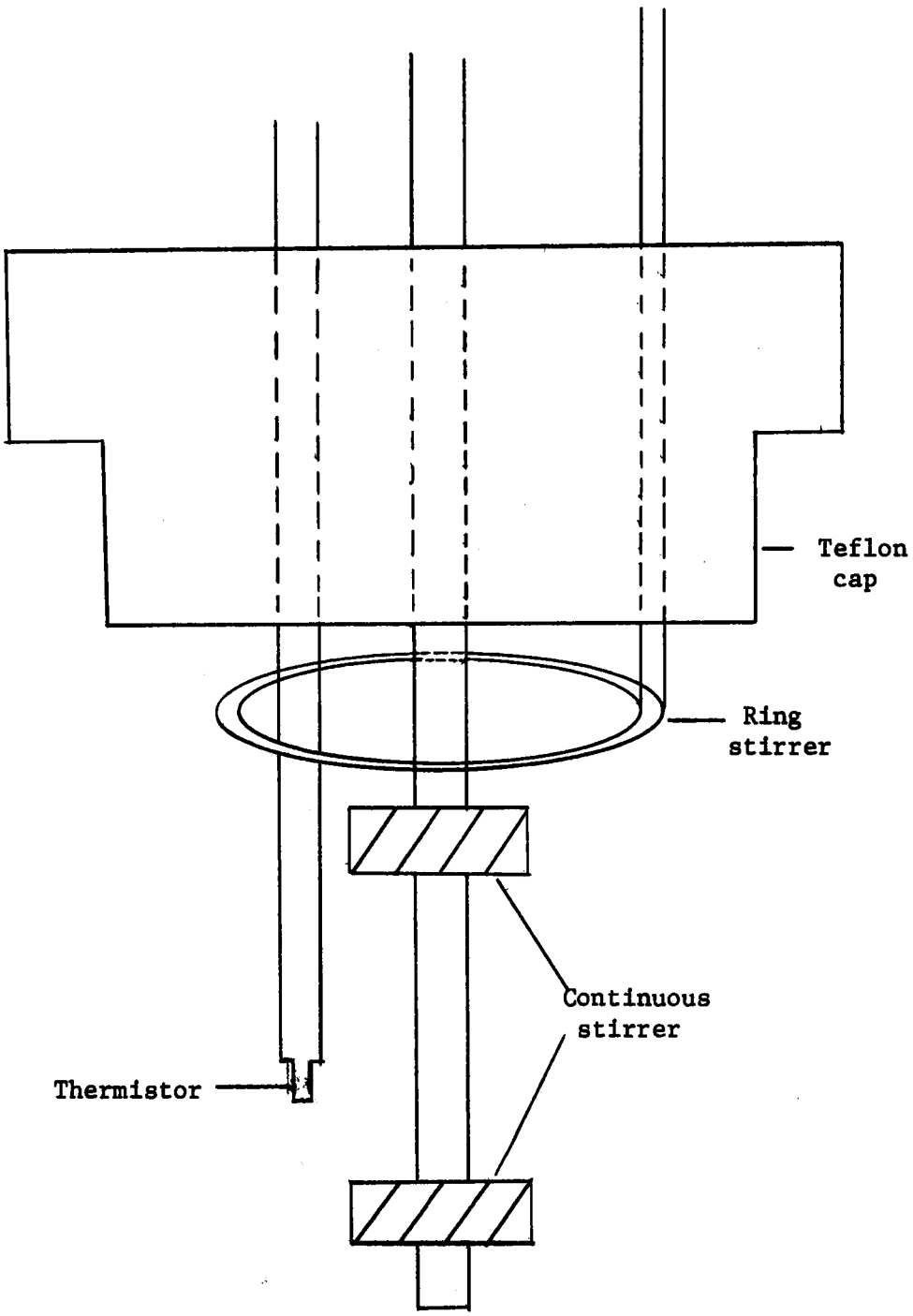

Figure 1. Freezing point apparatus.

3. The Temperature Scale

The thermal calibration of the thermistor is important. It was accomplished by making a careful comparison with the platinum resistance thermometer (T-1) in the Tronac constant temperature bath (p 20) which forms part of our isothermal calorimeter. The temperature control on this bath is very good — approximately $\pm$ 1 or 2 x 10^{-4}°K. The thermistor was calibrated at approximately every 0.4 degree between 267 and 290°K. The 1948 International Practical Temperature Scale was used. The thermometer resistances were measured with a Leeds and Northrup G-1 Mueller Bridge. The temperature-resistance readings are found in Appendix I, p 99. The least square analysis also reported there was based on the form[16]

$$R = A \exp (B/T + C/T^2) . \qquad (1)$$

T is the temperature in °K. From the statistics of the least squares fit, the precision of the temperature measurements is $\sim$ 2 x 10^{-5}°K. The accuracy is determined by the thermometer calibration and is no better than $\pm$ 0.001°K.

The platinum thermometer (T-1) used for the calibration of the thermistor had been calibrated[17] in this laboratory at the ice, steam, and sodium sulfate points. In order to be certain of this thermometer calibration, it was recalibrated against a second platinum thermometer at the Oak Ridge National Laboratory. The Oak Ridge thermometer was a secondary standard and traceable to the National Bureau of Standards. The results of the two thermometer calibrations were identical. The pertinent data are found in Appendix I.

Ten months after the first thermistor calibration, a second calibration was performed using platinum thermometer (T-1) and a second platinum thermometer (T-2) which had also been calibrated in this laboratory. The absolute temperatures calculated using the three thermistor calibrations differed by as much as 0.001°K which is the limit of precision of the Mueller Bridge used for the thermometer readings. For the calculation of a temperature difference of 0.03 degree (the smallest temperature change measured) the three thermistor calibrations agreed to within $\pm$ 5 x 10^{-6}°K or 0.02% (this precision was maintained or bettered over the entire experimental range). This procedure shows the thermistor to be stable over a relatively long time period and firmly establishes the temperature scale.

4. Determination of Concentration

The concentration of the NaCl solutions was determined by a method adapted from one originally suggested by Richards.[18] A sample ($\sim$ 5 to 10 ml) of the unknown solution was carefully weighed and added to a 250 ml beaker and diluted with H_2O to approximately 100 ml. The Cl^- was then titrated with a standard $AgNO_3$ solution added from a weighing buret. The progress of the titration was followed potentiometrically using an Orion Research pH meter. A standard glass electrode and a silver electrode were used as the reference and working electrode, respectively. Near the endpoint the $AgNO_3$ solution was deliberately exceeded by one or at most two drops of the $AgNO_3$ solution. The resulting precipitate and solution were heated to $\sim$ 90° to promote coagulation,[19] and the precipitate was aged overnight at room temperature. The precipitate was protected at all times from direct light to prevent reduction of Ag^+ to

Ag°. After the aging process was complete, some of the liquid was filtered, and the concentration of Ag^{+} in the supernatant determined by atomic absorption flame photometry using a Perkin Elmer Model 303 spectrophotometer equipped with a silver lamp. The instrument was calibrated before each day's run using a set of $AgNO_3$ standards, and a Beer's law plot prepared.

The calculation of the Cl^{-} concentration from the data was straightforward once account was taken of the AgCl solubility and the adsorption[20] of Ag^{+} on the precipitate. Both corrections were very small but became relatively larger as the Cl^{-} concentration decreased. The analytical technique was laborious but yielded concentration data good to better than $\pm$ 0.03% as determined by many replicate experiments. (A minimum of two determinations were made on each NaCl solution.) This was in agreement with our predictions. With 0.5% of the titrant in excess determined to 3% by atomic absorption, the error should be about 0.02% without allowing for any statistical error in the weighing of the buret. At Cl^{-} concentrations below 0.05 molal the precision was lower because the relative amount of Ag^{+} present as excess became larger.

The $AgNO_3$ solutions used as standards were standardized by titrating a known Cl^{-} solution using the above technique. A minimum of five determinations were made for each $AgNO_3$ solution, and the average standard deviation was 0.02%. The titrating solutions employed had nominal concentrations of 1.6, 2.5, 5.0, and 10.0 weight percent $AgNO_3$ depending on initial Cl^{-} concentration. The Beer's Law standards ranged from 2 to 50 ppm of Ag^{+}.

5. Errors

Most of the errors in the freezing point measurements have been discussed above. A summary is given in Table I.

TABLE I

ERROR ANALYSIS OF FREEZING POINT DATA

Error Source	% Error x 10^2
Thermistor calibration	2
Thermometer calibration	1
Analysis	3
Error in standards	2

The best previous freezing point measurements for NaCl in H_2O are those of Scatchard and Prentiss.[21] Comparison of their data with that of the present work (see p 63) showed that the two are within the combined experimental error except below 0.1 molal where the difference increases. The estimated errors in Scatchard and Prentiss's experiments are essentially identical to those of the present work. At 0.1 m the combined uncertainties are $\pm$ 0.001 osmotic units increasing to about $\pm$ 0.003 at 0.01 m. The reported differences are within 0.001 at 0.1 m but amount to 0.005 at 0.01 m. This is almost two times the estimated combined uncertainties (see p 63). This difference below 0.1 m led to a re-evaluation of our analytical technique. The distilled water was

rechecked for Cl^-, and the correction for absorption of Ag^+ was reexamined. Known Cl^- solutions were titrated to recheck the standardization of the $AgNO_3$ solutions, and known solutions at low Cl^- concentration (below 0.1 molal) were titrated to check the reliability of the technique. No systematic errors in the analytical technique could be found.

The freezing point of pure H_2O or D_2O is a function of the amount of dissolved air. The corresponding solubility of air in a salt solution is less than that in the pure solvent. This salting out effect is of concern because it can make a contribution to the observed freezing point depression. Calculations which are in agreement with those of Scatchard[14] show that the error in the observed freezing point depression caused by salting out of air is 0.003% at 1 molal and 0.006% at 2 molal (which is the highest concentration used in the present work). The errors become smaller at lower salt concentrations. This error is reduced by the compensating effect of air becoming more soluble as the temperature decreases. In any event the error caused by the two effects is negligible compared to other errors in temperature and concentration. It should be pointed out that the use of a second Dewar as a reference (freezing point of pure solvent) would have required that both Dewars be saturated with air or air free.

6. Isotopic Analysis

In the series of measurements using D_2O as a solvent, the concentration of the contaminant H was determined using a Varian A-60 nmr spectrometer. The instrument was calibrated before each run with a set of standards ranging from 99.0 to 99.8 mole percent D. This

method gave the mole percent of D in the sample to better than 0.1%. The measured isotope effects were then corrected to 100% D_2O as described below (p 67).

The D_2O used in the freezing point measurements was recovered by distilling the solutions using a Nester Faust spinning band column. The concentration of H never exceeded 0.8 mole percent.

7. Experimental Procedure

In a typical experiment the Dewar was filled about two thirds full with finely crushed H_2O or D_2O ice prepared by freezing the pure solvents in thin polyethylene bags. The remainder of the vessel was filled with pure solvent. The teflon cap containing the stirrers and thermistor was then inserted and the entire assembly placed in a water bath maintained at approximately the freezing point of the pure solvent. The stirrer was started and the voltage of the mercury cell measured using the K-4 potentiometer. A constant base line was established ($\pm$ 2 x 10^{-5}°K) and then solid NaCl or a concentrated solution added. (In runs with D_2O only thoroughly dried solid was added to minimize possible H_2O contamination. If H_2O were added with the sample, an error would result because of the isotope effect on the solvent freezing point.) After the NaCl was added, a new temperature equilibrium was established within several minutes. The bridge voltage was read and a sample of the solution taken. More NaCl was then added, and the procedure repeated. No more than three concentration runs were made for each filling of the Dewar with ice and solvent. When D_2O was the solvent, a sample was taken and analyzed for H_2O.

The thermal base lines for solution in equilibrium with solid solvent shifted slightly with time because of the small amount of melting caused by the heat of stirring. The resultant concentration change causes the temperature to rise slightly, but under the conditions of the experiment this is easily corrected for and has been carefully considered in our data analysis.

C. Calorimetry: Apparatus and Procedures

1. Calorimetric Experiments

In order to employ osmotic coefficients and isotope effects on osmotic coefficients derived from freezing point measurements they must be corrected to a standard temperature. This is because the experimentally observed quantities refer to the freezing point of the solutions which are functions of the concentration and of the isotopic analysis. The correction requires information on the temperature and concentration dependence of the solvent activity which in turn can be expressed in terms of the partial molal enthalpy of the solvent. Therefore, information on heats of solution and dilution of NaCl in H_2O and D_2O is needed.

The first part of our calorimetric program was concerned with the measurements of heats of dilution as a function of temperature and concentration in each isotopic solvent. This work was carried out in a submersible adiabatic calorimeter designed and built in this laboratory. After more precise and convenient calorimetric equipment became available, it was employed in a series of measurements of the differential heats of solution of NaCl (crystal) in solutions of NaCl in H_2O or D_2O, again as functions of concentration and temperature. These measurements

allow calculation of the relative partial molal enthalpy of the solvent by use of standard thermodynamic techniques (p 37).

2. Adiabatic Calorimetry

a. Design. Each of the twin submersible adiabatic calorimeters built in this laboratory consisted of a glass Dewar vessel ($\sim$ 20 cm^3) fitted with a teflon cap. The teflon cap mounted a glass probe thermistor (Veco #32A1, 2000 nominal ohms at 25°), a precision wire wound electrical heater (100 ohms), a glass stirring rod, a glass rod serving as a bulb crusher, and a 1 mm copper wire in thermal contact with a Peltier cooler. A schematic is shown in Figure 2. The stirring rod and bulb crusher entered through '0' ring seals to prevent loss of solvent and/or contamination of D_2O with atmospheric water. The thermistor was used to monitor temperature changes in the vessel and served as one leg of a dc Wheatstone bridge. The other three legs of the bridge were precision resistance boxes (Leeds and Northrup) fitted with wire wound (low temperature coefficient) resistors and stored in a thermally insulated box. The temperature sensitivity of the system was better than 1×10^{-4}°K.

The Peltier cooler (Borg-Warner Corp., no. 930-7) was powered by a stabilized power supply which was continuously adjustable over the useful range of the unit. Its purpose was to allow a rapid adjustment of the initial temperature of the calorimeter to the external bath temperature and/or to cancel excessive heats of stirring during a run.

b. Thermal calibration. Since the total heat capacity of the system was generally different for each run, it was necessary to include

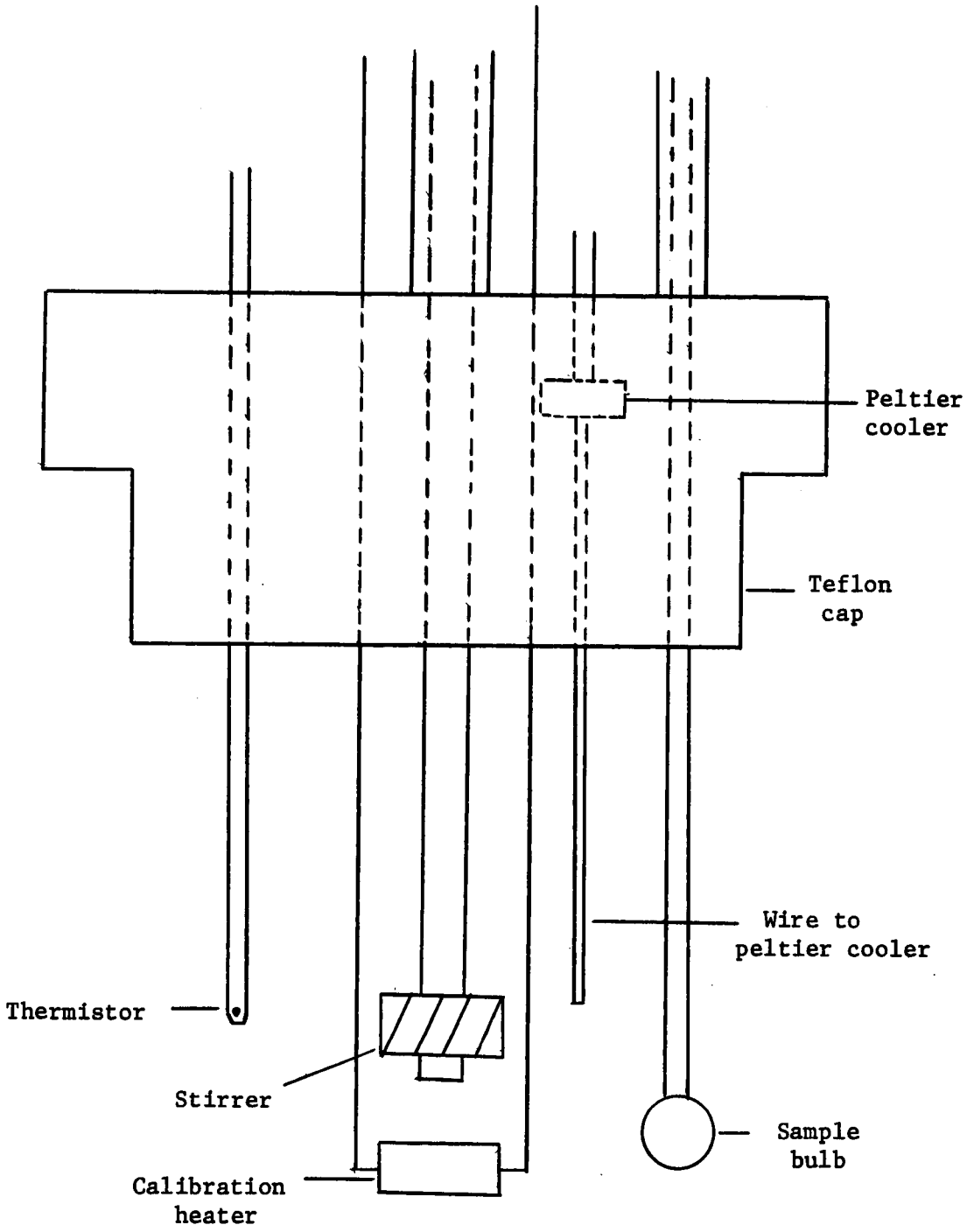

Figure 2. Adiabatic calorimeter.

a thermal calibration step in each series. The calibrating heater circuit consisted of a precision heater, a standard resistor, a precision power supply (Princeton Applied Research Model No. 157), and a timer (± 0.01 sec, A. W. Haydon Company Model No. K15140). The heater and standard resistor were 100 and 9.9898 ohm (25°) wire wound resistors, respectively.

The resistance of the heater was measured and rechecked periodically by use of a calibrating circuit in which the standard resistor and heater were in series with a precision power supply. The potential drop across each resistor was measured with the K-4 potentiometer. The resistance of the heater was determined by multiplying the ratio of potentials by the resistance of the standard resistor. Several different heaters (nominally 100 Ω) were employed. Their resistances were measured to ± 0.01 Ω.

In a calibration run the timer and energy input to the heater are started simultaneously using a precision double pole double throw switch, and while the calibration was in progress the potential drop across the standard resistor was measured with the K-4 potentiometer. The heat input to the vessel is

$$q_c = (E_s R_s^{-1})^2 R_h t_c \qquad (2)$$

where q_c is the heat added in joules, E_s is the potential drop across the standard resistor, R_s is the resistance of the standard resistor, and t_c is the time (sec) which the heater circuit operates. A minimum of two calibrations were performed for each heat measurement.

c. Experimental procedure. The adiabatic calorimeter was used to measure integral heats of solution and heats of dilution. In a run

a thin walled glass sample bulb was weighed and filled with either dry crystalline salt or a solution of known composition and sealed with a small flame. Liquid samples were added to the bulb with a syringe. To help prevent loss of solvent from the bulb during sealing, the solution was first frozen in a trichloroethylene-Dry Ice bath. The bulb was then sealed and allowed to return to room temperature before being placed in a desiccator. The bulb was reweighed after drying and was then attached to the bulb crusher and placed in the calorimeter.

The twin adiabatic calorimeter vessels described above were immersed in a water bath controlled to $\pm$ 0.01°K. Either the Peltier cooler or the heater was used to bring the vessels to the desired temperature. To insure maximum bridge sensitivity the three resistance boxes in the Wheatstone bridge were adjusted to roughly the same resistance as the thermistor. Usually one calibration was performed before, and a second after, the sample bulb was broken. The time versus temperature curves for the calibration and the run were recorded. A typical plot is shown in Figure 3. The major differences between the curve for a run and a calibration are that one was exothermic (calibration) and the other was endothermic (run), and also that the heating rate for a run was usually larger than that for a calibration.

In Figure 3 note that Line A and B are very nearly straight while C roughly follows Newton's Law of Cooling which describes the return of the vessel to the bath temperature. The quantity of experimental interest in Figure 3 is the length of Line D which graphically shows the temperature change for the experiment.

A computer program was written to aid in the calculation of the length of Line D. The coordinates of six points from Line A, three

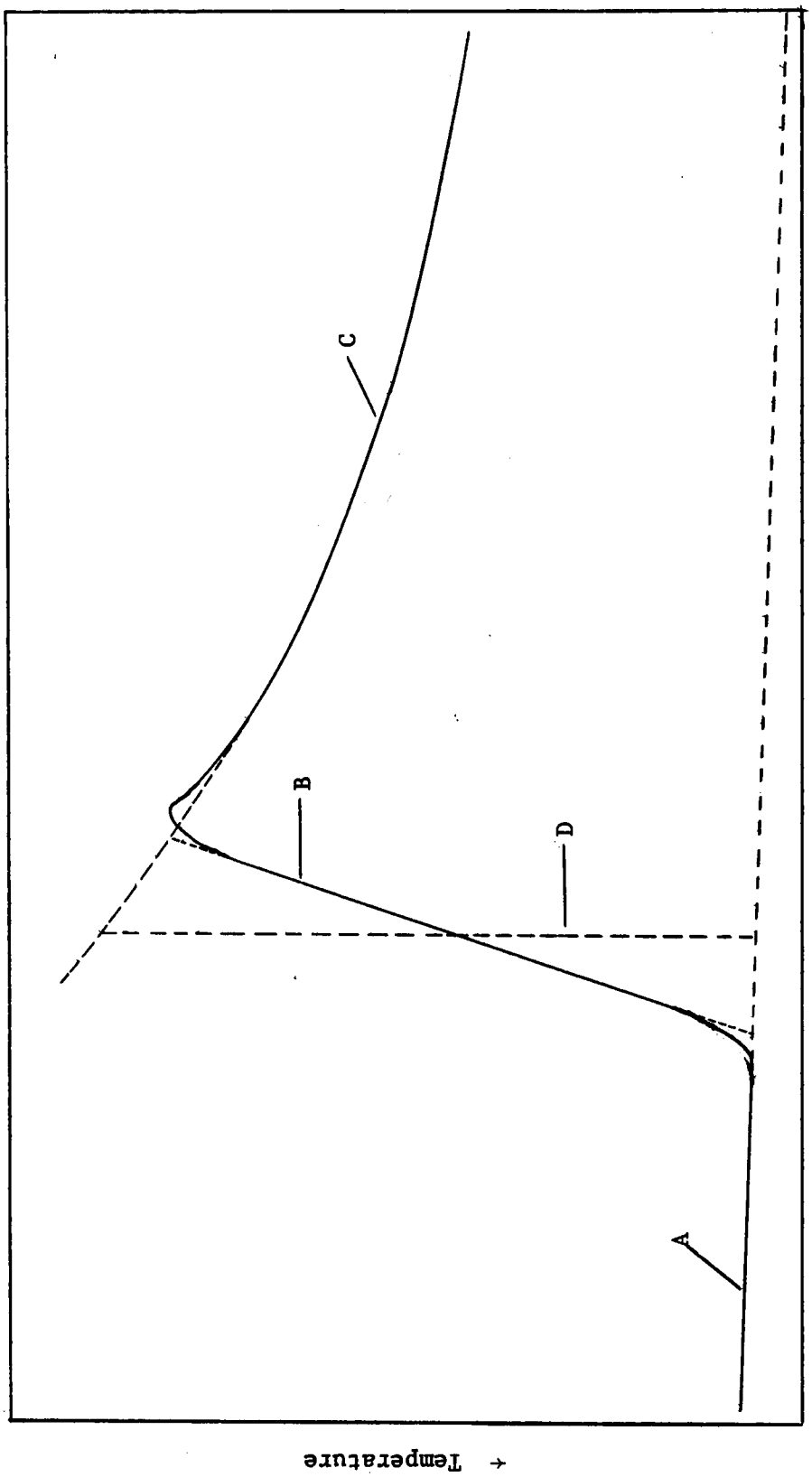

Figure 3. Temperature vs. time plot for adiabatic calorimeter.

from Line B, and eight from Line C were fed into the program. The points were taken at one minute intervals for Lines A and C, and equidistant along Line B. In order to eliminate the effects of recorder overshoot, finite mixing times, etc., no points were taken from Line C until the smooth region passed the overshoot. This region usually occurred from two to three minutes after the calibration heater was turned off or after the breaking of the sample bulb. Using a least-squares computer program[22] Lines A and B were fit to a straight line and C was fit to a relation derived from Newton's Law:

$$\ln \frac{(T_C-T_A)_2}{(T_C-T_A)_1} = -k(t_2-t_1) \quad . \tag{3}$$

T_C-T_A is the difference between the relative temperature of Line C and the extrapolated relative temperature of Line A. The subscripts 1 and 2 refer to any two times, t_1 and t_2, and k is a proportionality constant determined in the fit. With the equations for all three lines, the program solves for the intersections AB and BC and averages the time coordinates to determine the point of inflection. The abscissa of this point is now substituted into the equations for Lines A and C and the length of Line D obtained. With results for both the run and calibrations the chemical heat is obtained by

$$q_r = q_c \left(\frac{D_r}{D_c} \right) \quad . \tag{4}$$

The subscript r refers to the run and c to the calibration.

All chemical heats were corrected for the heat of bulb breaking which was independently determined as $- 0.02 \pm 0.01$ cal.

d. Errors. The adiabatic calorimeter yields heats good to about 1%. The main errors are the uncertainty in the heat of bulb breaking and the error in reading the relative temperatures from the recorder chart.

3. Isothermal Calorimetry

a. Design. The isothermal calorimeter used in the present work was a commercially available Tronac Model 550 Isothermal Calorimeter. The calorimeter was purchased from Tronac Inc. of Orem, Utah.

A schematic of the reaction vessel is shown in Figure 4. This double walled vessel was constructed of stainless steel and contained two thermistors, a calibration heater and a stirrer. At the base of the inner vessel and physically situated in the cavity between the inner and outer walls but in physical contact with each are a control heater and a Peltier cooler. The electronics and principles of operation were centered around two Wheatstone bridges.

The monitor thermistor was one leg of a dc Wheatstone bridge and served as an internal thermometer. Prior to an experiment the monitor thermistor was immersed in the water bath, and the other resistances in the bridge were adjusted to null the output voltage within the thermal noise level of the bath. The Tronac bath had a short term stability of $\pm$ 2 x 10^{-4}°K.which corresponded to $\sim \pm 5\mu$ volts in the bridge output. The absolute temperature of the bath was measured to $\pm$ 0.001°K with a platinum resistance thermometer.

After the vessel was assembled and placed in the bath, its temperature was adjusted.so that the output of the monitor bridge

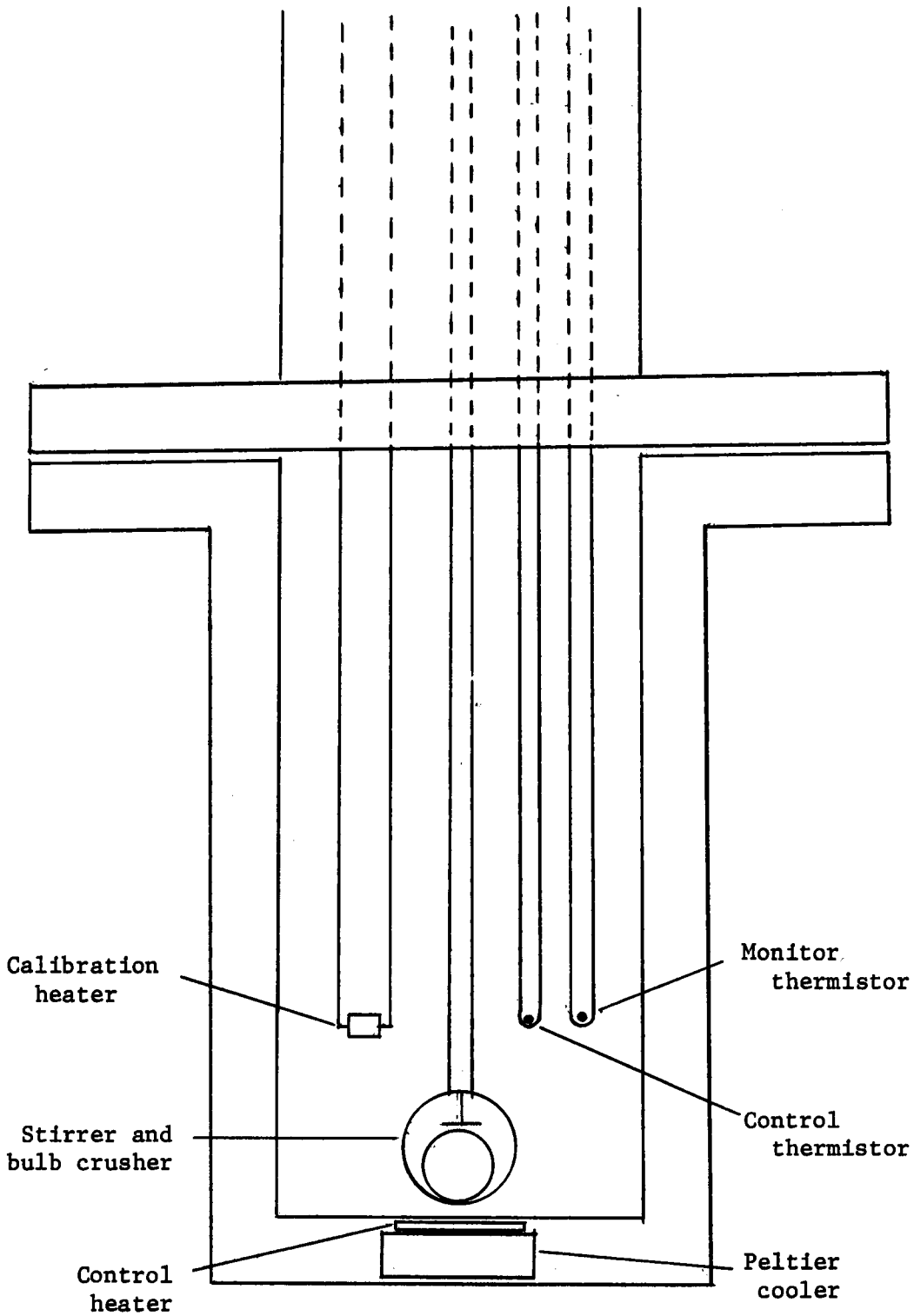

Figure 4. Isothermal calorimeter vessel.

was zero. The control thermistor formed one leg of an ac phase sensitive Wheatstone bridge. The other resistances of the control bridge were adjusted to maintain the temperature inside the vessel at the bath temperature. The voltage output of the control bridge was proportional to the temperature difference $(T_{bath}-T_{vessel})$. The function of the control circuitry was to minimize this error signal. To that end the voltage from the control bridge was amplified and used to control the amount of power supplied to the control heater. That power was supplied via a capacitative charge-discharge cycle. The number of pulses per sec was monitored and formed the pertinent experimental information. The Peltier cooler was adjusted so that the heater had to be pulsed a finite number of times per sec in order to maintain the temperature at the set point. The control heater could be pulsed up to 24,000 times a second, and thus the Peltier cooler was adjusted to give an appropriate pulse rate prior to an experiment.

As in the case of the adiabatic calorimeter, an electrical calibration had to be performed on the isothermal calorimeter. The calibration heater circuit was basically of the same design as that described for the adiabatic calorimeter (p 14). The only differences were that no timer was needed and that the potential drops across the standard resistor and calibration heater were measured by a Data Technology Multimeter. Although calibration procedures for the adiabatic and isothermal calorimeters were similar, it should be recognized that two entirely different quantities are under consideration. In the calibration of the adiabatic calorimeter, the heat capacity of the vessel plus contents was determined, while the

calibration of the isothermal calorimeter determined the energy per pulse delivered to the control heater. The isothermal calorimeter thus had the advantage that a separate calibration was not necessary for each experiment.

b. Experimental procedures. In a typical experimental run, a constant base line of pulses per second was established. A thin walled glass sample bulb ($\sim$1 cm^3) was then broken by a spring loaded plunger. If the chemical heat was exothermic, fewer pulses were needed to keep the temperature constant. Conversely, more pulses were required if the chemical heat was endothermic.

It was necessary to determine the total number of heater pulses for the period of the reaction and to subtract the number of pulses which would have been necessary to maintain a constant temperature if no reaction had taken place. This difference multiplied by the energy per pulse gave the chemical heat of the reaction.

The raw heat datawere corrected for the heat of bulb breaking which was found to be -0.005 ± 0.004 cal. The heat of bulb breaking was not the same as that obtained for the adiabatic calorimeter because the physical characteristics of the bulb breaking systems were quite different.

The chemical heats were also corrected for the nonisothermal behavior of the system. When a chemical heat was produced, the temperature of the reaction vessel changed slightly before the electronics could restore the temperature to the control point. During the brief temperature excursion, heat could either enter or leave the

reaction vessel via paths other than the Peltier cooler-control heater loop. This heat leakage was determined by recording the output of the monitor bridge. A typical temperature time plot is shown below for an endothermic heat measurement. Area A corresponds to the vessel being

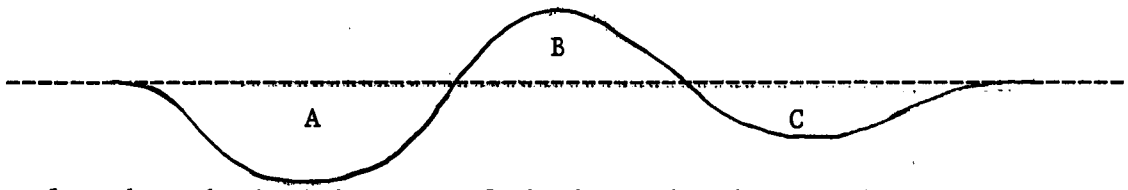

cooler than the bath because of the heat absorbed by the chemical reaction. Heat therefore entered the vessel from the bath. Area B results from a slight overshoot by the control circuitry causing the temperature of the vessel to be higher than that of the bath. Heat flowed out of the vessel during this time. Area C is due to a small undershoot and resulted in heat again entering the vessel. Areas A + C - B give a measure of the net heat which (in this example) entered the vessel. To convert the area to the amount of heat gained, it was necessary to multiply by the thermal conductivity of the vessel. The thermal conductivity ($\frac{\text{cal/sec}}{\text{chart unit}}$) was determined by changing the temperature of the vessel so that it was slightly different from the bath. The difference in the pulsing rate and the displacement on the recorder chart was noted. The heat per sec was calculated from the change in the pulsing rate. This was divided by the recorder displacement to give the required thermal conductivity. The correction was not negligible and at times amounted to several percent of the observed chemical heats.

The isothermal calorimeter was used to measure differential heats of solution of NaCl in NaCl solutions of H_2O and D_2O.

c. Error. This isothermal calorimeter is capable of measuring heats to about 0.1%. However, the precision of the measured heats in the present series is only about 1% due to the uncertainty in the heat of bulb breaking, and the error in correcting for the nonisothermal behavior of the system. Although heats of dilution could have been measured with greater precision using the isothermal calorimeter, they would have been laborious. The convenience of differential heat of solution measurements far outweighed the gain in precision which would have resulted from dilution studies.

CHAPTER III

RESULTS

A. Background

All of the results obtained in the present investigation have been smoothed and later interpreted within the framework of one or more forms of the extended Debye-Hückel theory. Smoothing was done with the Lietzke nonlinear least-squares routine.[22] Before presenting the detailed experimental results it is appropriate to show the essentials of the equations which result from the extended Debye-Hückel treatment.

The equation originally derived by Debye and Hückel[23,24] for the mean activity coefficient is given by

$$\ln\gamma_{\pm} = \frac{-S\sqrt{I}}{1+A\sqrt{I}} \quad . \tag{5}$$

The ionic strength, I, is defined by

$$I = 1/2 \sum_i m_i Z_i^2 \quad , \tag{6}$$

where Z_i is the formal charge and m_i is the aquamolality of an ionic species i. The aquamolality is a concentration scale[12] expressed as moles of solute per 55.508 moles of solvent. S is the limiting slope (infinite dilution) and is given as

$$S = \frac{-e^2\kappa(Z_+Z_-)}{2\varepsilon kT} \quad . \tag{7}$$

Here e is the charge on the electron, Z_+ and Z_- are formal charges, T

is the Kelvin temperature, ε is the dielectric constant, k is the Boltzmann constant, and κ is

$$\kappa = \left(\frac{4\nu\pi e^2 N o d_1}{\omega \varepsilon k T} \right)^{1/2} . \qquad (8)$$

No is Avogadro's number, d_1 is the density of the solvent, ω is the weight of 55.508 moles of solvent, and ν is the number of moles of ions per mole of solute.

The quantity A in Equation 5, p 26, is given as $A = a^\circ\kappa$ where a° is a parameter which has been interpreted[23,24] as the average distance of closest approach of positive and negative ions in solution. Harned and Owen[25] give an excellent discussion of the basis of this interpretation.

The original Debye-Hückel theory, Equation 5, is useful only at very low ionic strength. Hückel[26] extended the theory by adding a term. He reasoned that the dielectric constant of the solvent varied linearly with ionic concentration and approximated the consequences by adding a term, BI, to Equation 5. Since that time more empirical terms have been added and one form of the extended Debye-Hückel theory is given by Equation 9.

$$\ln \gamma_{\pm} = \frac{S\sqrt{I}}{1 + A\sqrt{I}} + BI + CI^2 + DI^3 + \text{---} \qquad (9)$$

B, C, and D are parameters, and their temperature dependence can be assumed to have the general form[27]

$$B = B_1/T + B_2 \ln T + B_3 + B_4 T . \qquad (10)$$

In the present work one modification of the commonly employed definition of κ was made. Since the term $\nu N o d_1 \omega^{-1}$ is the limiting

number of ions per cm^3, it seemed appropriate to set $d_1 = d_s$, the density of the solution. In that case, ω must be replaced by ω_s which is the weight of 55.508 moles of solvent plus the weight of the solute.

Equations in terms of the extended Debye-Hückel theory can also be derived for other thermodynamic properties of interest. The osmotic coefficient, ϕ, as defined by Bjerrum[28] can be expressed

$$\phi = 1 + \frac{1}{m} \int_0^m m \, d\ln \gamma_{\pm} \tag{11}$$

When Equation 9 is differentiated, substituted in Equation 11, and the integration performed, Equation 12 results.[27,29,30]

$$\phi = 1 - \frac{S}{A^3 I} \left(\beta - 2\ln\beta - \frac{1}{\beta}\right) +$$

$$(1/2)BI + (2/3)CI^2 + (3/4)\,DI^3 + \text{---} \tag{12}$$

Here $\beta = 1 + AI^{1/2}$.

The relative partial molal enthalpy of the solute, $\bar{L}_2$, is given by

$$\bar{L}_2 = -\nu RT^2 \left(\frac{\partial \ln \gamma_{\pm}}{\partial T}\right) . \tag{13}$$

(Throughout this paper the solute will be denoted by a subscript 2 and the solvent by the subscript 1.)

The rather complicated result is shown in Equation 14,

$$\bar{L}_2 = \nu RT^2 \left[Q_1 \left(-\frac{2d\ln a^\circ}{dT} + \alpha + \frac{1}{T} + \frac{d\ln\varepsilon}{dT}\right)\right.$$

$$+ Q_2 \left(\frac{\alpha}{3} + \frac{1}{T} + \frac{d\ln\varepsilon}{dT}\right) +$$

$$\left(\frac{dB}{dT} - B\alpha\right)I + \left(\frac{dC}{dT} - 2C\alpha\right)I^2 +$$

$$\left.\left(\frac{dD}{dT} - 3D\alpha\right)I^3 + \text{---}\right] . \tag{14}$$

Q_1 and Q_2 are given by:

$$Q_1 = \frac{Z_+ Z_- e^2 \kappa^2 a^\circ I}{4\varepsilon kT(1 + \kappa a^\circ \sqrt{I})^2} \quad , \tag{15}$$

and

$$Q_2 = \frac{-3\kappa e^2 \sqrt{I}}{4\varepsilon kT(1 + \kappa a^\circ \sqrt{I})} \quad . \tag{16}$$

Here α is the coefficient of thermal expansion for the solution and results from the differentiation of the density with respect to temperature.

Equations for ϕ and $\bar{L}_2$ were derived from Equation 9, p 27, using the density of the solvent. If the density of the solution (which is a function of concentration) is used, slightly different expressions would have resulted. However, sample calculations show that the difference is small (at most a few percent of the value of the Bm term) and is compensated for by the empirical adjustment of the higher order terms in the data fitting process.

It should be emphasized that the terms in Equations 9, 12, and 14, p 28, which contain the parameters B, C, and D are purely empirical. The equations which result when these parameters are set to zero contain only the terms which are derived from the theoretical treatment of Debye and Hückel. In the present work these terms which result from the theoretical derivation will be referred to as the DH terms. For example, the DH term for the mean activity coefficient is given by Equation 5, p 26.

In all the fits using the Debye-Hückel theory, the density of the H_2O and D_2O solutions was calculated by using the partial molal

volumes of Millero,[31] the isotope effect (IE) on the partial molal volumes reported by Choi and Bonner,[32] and the density of the pure solvents given by Kell.[33] The dielectric constants of the solvents, H_2O and D_2O, were taken from the data of Vidulich, Evans, and Kay.[34]

B. Enthalpies

1. H_2O Data

The measured differential heats of solution, ΔH_H^{df}, of NaCl in its H_2O solutions are presented in Table II. The aquamolality, m (p 26), refers to the average concentration of the solution. When thermodynamic properties are compared in different solvents, this scale assures that comparisons are made at equal mole fractions. The data in Table II were taken with the Tronac isothermal calorimeter by adding a small quantity (Δn moles) of solid salt to a solution of original concentration, m- ($\Delta m/2$). The experimental ratio, $q_{obs}/\Delta n$, is thus to a good approximation a direct measure of the differential heat of solution, ΔH_H^{df}. The approximation becomes better as Δn (and correspondingly Δm) decreases. For the reported measurements Δm was invariably 0.018 and corresponded to the addition of 0.026 g of NaCl to 25 cm^3 of solution.

The relative partial molal enthalpy, $\bar{L}_{2H}$, of NaCl can be expressed as

$$\bar{L}_{2H} = \Delta H_H^{df} + L_{2H}^{s} , \qquad (17)$$

where L_{2H}^{s} is given by

$$L_{2H}^{s} = H_{2H}^{s} - \bar{H}_{2H}^{\circ} . \qquad (18)$$

TABLE II

EXPERIMENTAL VALUES OF ΔH_H^{df} AND $\bar{L}_{2H}$ for NaCl IN H_2O[a]

t, °C	m	ΔH_H^{df}	$\bar{L}_{2H}$
5	0.009	1692	34
	0.111	1662	4
	0.111	1663	5
	0.513	1376	-282
	0.513	1376	-282
	1.01	1037	-621
	1.01	1038	-620
	2.02	503	-1155
	2.02	503	-1155
	4.05	72.9	-1585
	4.05	72.9	-1585
15	0.0093	1288	43
	0.0101	1290	45
	0.110	1296	51
	0.110	1296	50
	0.513	1107	-138
	0.492	1117	-128
	1.01	865	-380
	1.01	864	-380
	2.02	473	-772
	2.01	477	-768
	4.06	133	-1112
	4.01	133	-1111
25	0.0100	969	55
	0.0111	971	57
	0.1105	1006	93
	0.1115	1006	93

TABLE II (Continued)

t, °C	m	ΔH_H^{df}	$\bar{L}_{2H}$
	0.5135	897	-17
	0.5142	896	-18
	1.014	733	-181
	1.018	731	-183
	2.030	462	-453
	2.029	462	-453
	4.063	225	-689
	4.093	224	-690
40	0.0094	545	70
	0.1100	623	148
	0.5144	595	120
	1.014	511	36
	2.019	370	-106
	4.042	308	-167

[a]Units are cal $mole^{-1}$.

Here H_{2H}^{s} and $\bar{H}_{2H}^{\circ}$ are the enthalpy of the solid salt and the partial molal enthalpy of the salt at infinite dilution, respectively. Thus, L_{2H}^{s} is the negative of the integral heat of solution at the infinite dilution limit (heat produced when one mole of salt is added to an infinite amount of solvent). Values of $\bar{L}_{2H}$ calculated using the L_{2H}^{s} values of Criss and Cobble[35] are given in Table II.

2. Fitting of $\bar{L}_{2H}$

An equation for $\bar{L}_{2H}$ as a function of temperature and concentration is of use. The data in Table II together with the bulk of the available literature data,[36-38] Table III, were fit to Equation 14 (p 28). The parameter D was set equal to zero, and the value of the a° parameter for NaCl in H_2O obtained from activity coefficient data,[25] a_H° = 4.2 A°, was employed. The a° parameter was assumed to be temperature independent: $(\partial \ln a_H^{\circ}/\partial T)$ was set equal to zero. The values of the parameters obtained from the fit are:

$$B_1 = -7.66960 \times 10^{3} \pm 8.9464 \times 10^{2},$$

$$B_2 = -4.72705 \times 10^{1} \pm 5.8684 \times 10^{0},$$

$$B_3 = 2.73593 \times 10^{2} \pm 3.3413 \times 10^{1},$$

$$B_4 = 7.38198 \times 10^{-2} \pm 9.5526 \times 10^{-3},$$

$$C_1 = 1.45640 \times 10^{3} \pm 3.9743 \times 10^{2},$$

$$C_2 = 9.33307 \times 10^{0} \pm 2.59753 \times 10^{0},$$

$$C_3 = -5.36058 \times 10^{1} \pm 1.48424 \times 10^{1},$$

and $$C_4 = -1.51202 \times 10^{-2} \pm 4.2126 \times 10^{-3}.$$

The variance of fit was 1.89×10^{2}. This fit is used in subsequent calculations involving $\bar{L}_{2H}$. A graph of the concentration dependence of $\bar{L}_{2H}$ at 5, 15, 25, and 40° is shown in Figure 5.

TABLE III

LITERATURE VALUES OF $\bar{L}_{2H}$ [a]

t, °C	m	$\bar{L}_{2H}$	Reference
15	0.0005	12.0	36
	0.001	16.5	
	0.005	35.8	
	0.010	46.0	
	0.050	65.0	
	0.100	57.7	
	0.200	9.4	
	0.404	-89.9	
25	0.00278	32	37
	0.00555	45	
	0.0111	59	
	0.0185	70	
	0.0555	93	
	0.10	97	38
	0.20	78	
	0.30	50	
	0.60	-50	
	0.90	-152	
	1.5	-333	
	2.0	-445	
	2.5	-551	
	3.0	-621	
	3.2	-642	
	3.6	-673	
	4.0	-688	
	4.4	-690	
	4.8	-677	
	5.0	-665	

TABLE III (Continued)

t, °C	m	$\bar{L}_{2H}$	Reference
40	0.10	148	38
	0.20	159	
	0.40	143	
	0.70	94	
	1.0	40	
	1.5	-41	
	2.0	-106	
	2.5	-151	
	3.0	-176	
	3.2	-180	
	3.5	-180	
	3.8	-173	
	4.2	-152	
	4.6	-119	
	5.0	-74	

[a]Units are cal $mole^{-1}$.

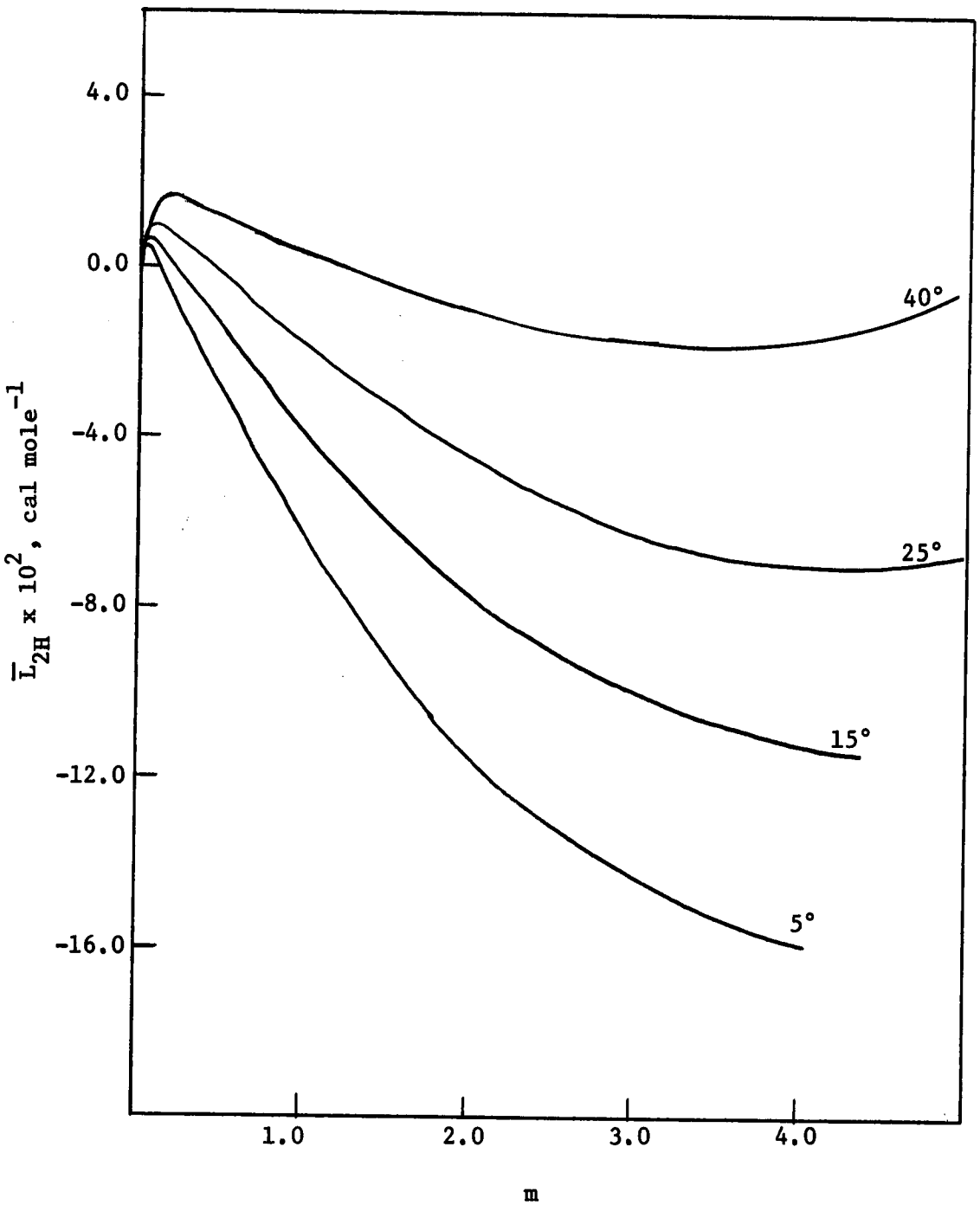

Figure 5. Plot of $\bar{L}_{2H}$ as a function of m.

The values of $\bar{L}_{2H}$ (Table III, p 34) taken from the literature were all determined by heat of dilution measurements while the present results are deduced from differential heats of solution. The agreement is good with the difference between the two methods usually being less than 10 cal mole^{-1}. Although somewhat more precise data can normally be obtained from dilution measurements, the technique is laborious and requires large quantities of solvent. It was therefore not applicable to the present study because the ultimate interest is in the properties of D_2O as solvent.

A second fit of the $\bar{L}_{2H}$ data was made in which $(\partial \ln a^\circ_H/\partial T)$ was taken as an adjustable parameter obtaining $(\partial \ln a^\circ_H/\partial T) = -6.7 \times 10^{-6} {}^\circ K^{-1}$. There was no improvement in the fit (the variance of fit was 1.92×10^2). Using a similar procedure, Gier and Vanderzee[39] determined $(\partial \ln a^\circ_H/\partial T)$ for HI to be $-2.7 \times 10^{-4} {}^\circ K^{-1}$. $(\partial \ln a^\circ_H/\partial T)$ for the two fits differs by a factor of about 40 while a°_H differs by a factor of only 1.4. Additionally, recall that for the NaCl case the introduction of $(\partial \ln a^\circ_H/\partial T)$ parametrically does not improve the fit. Also it is questionable as to just what physical significance can be attached to $(\partial \ln a^\circ_H/\partial T)$. Therefore, the earlier fit with $(\partial \ln a^\circ_H/\partial T) = 0$ is to be preferred.

3. Calculation of $\bar{L}_{1H}$

Values of the relative partial molal enthalpy, $\bar{L}_{1H}$, of H_2O will be of use later in this work. These can be obtained from the Gibbs-Duhem integration.

$$\bar{L}_{1H} = -\frac{1}{55.508} \int_0^m m \, d\bar{L}_{2H} \qquad (19)$$

Because of the involved concentration dependence of $\bar{L}_{2H}$, the value of the integral in Equation 19 was determined numerically. A computer program employing Simpson's Rule[40] was used to perform the integration. Calculated values of $\bar{L}_{1H}$ and $\bar{L}_{2H}$ at rounded temperatures and concentrations are given in Appendix II.

Although the dilution data of Young and Machin[41] could not be directly employed in the fits of $\bar{L}_{2H}$, they can be used to calculate values of $\bar{L}_{1H}$ at 0° which can then be compared with those predicted by Equation 19. The agreement is good with the largest difference being only 4%.

4. D_2O Data and Isotope Effects

Differential heats of solution in D_2O, ΔH_D^{df}, were measured under conditions which were identical to the measurements in H_2O. The experimental results are given in Table IV. There are no literature values for L_{2D}^{s} as a function of temperature. This prohibits the direct calculation of $\bar{L}_{2D}$. However, the quantity $\bar{L}_{2H}-\Delta H_D^{df}$ will be useful and is given in the table.

Values of $\bar{L}_{2H}-\Delta H_D^{df}$ plotted against $\sqrt{m}$ (Figure 6) appeared to be linear within the experimental error of the data. It should be noted that the concentration dependence of $\bar{L}_{2H}-\Delta H_D^{df}$ is the same as $\bar{L}_{2H}-\bar{L}_{2D}$ since L_{2D}^{s} is not a function of concentration. The data in Table IV were least-squared using Equation 20,

$$\bar{L}_{2H}-\Delta H_D^{df} = (a + bT + cT^2) + (d + eT)\sqrt{m} \quad . \qquad (20)$$

The quantity $(a + bT + cT^2)$ corresponds to L_{2D}^{s}, and $\Delta\bar{L}_2$ is given by

TABLE IV

EXPERIMENTAL VALUES OF ΔH_D^{df} AND $(\bar{L}_{2H}-\Delta H_D^{df})^a$

t, °C	m	ΔH_D^{df}	$\bar{L}_{2H}-\Delta H_{2D}^{df}$
5	0.0093	2618	-2584
	0.111	2560	-2555
	0.110	2554	-2549
	0.513	2129	-2411
	0.514	2159	-2441
	1.02	1679	-2300
	1.01	1664	-2285
	2.02	1078	-2233
	2.02	1059	-2214
	4.05	509	-2094
	4.05	460	-2045
15	0.0093	1991	-1947
	0.0100	2004	-1960
	0.110	2044	-1993
	0.111	1992	-1941
	0.513	1717	-1850
	0.492	1721	-1854
	1.021	1388	-1768
	1.01	1386	-1766
	2.03	925	-1695
	2.02	961	-1731
	4.06	490	-1602
	4.02	505	-1617
25	0.0100	1548	-1492
	0.0111	1534	-1478
	0.111	1493	-1400
	0.112	1536	-1443
	0.514	1378	-1396

TABLE IV (Continued)

t, °C	m	ΔH_D^{df}	$\Delta \bar{L}_{2H} - H_{2D}^{df}$
	0.514	1360	-1378
	1.01	1177	-1359
	1.02	1189	-1371
	2.03	849	-1302
	2.03	857	-1310
	4.06	536	-1225
	4.09	560	-1250
40	0.009	1007	-937
	0.110	1085	-937
	0.514	979	-859
	1.01	958	-922
	2.02	670	-776
	4.04	609	-776

[a]Units are in cal $mole^{-1}$.

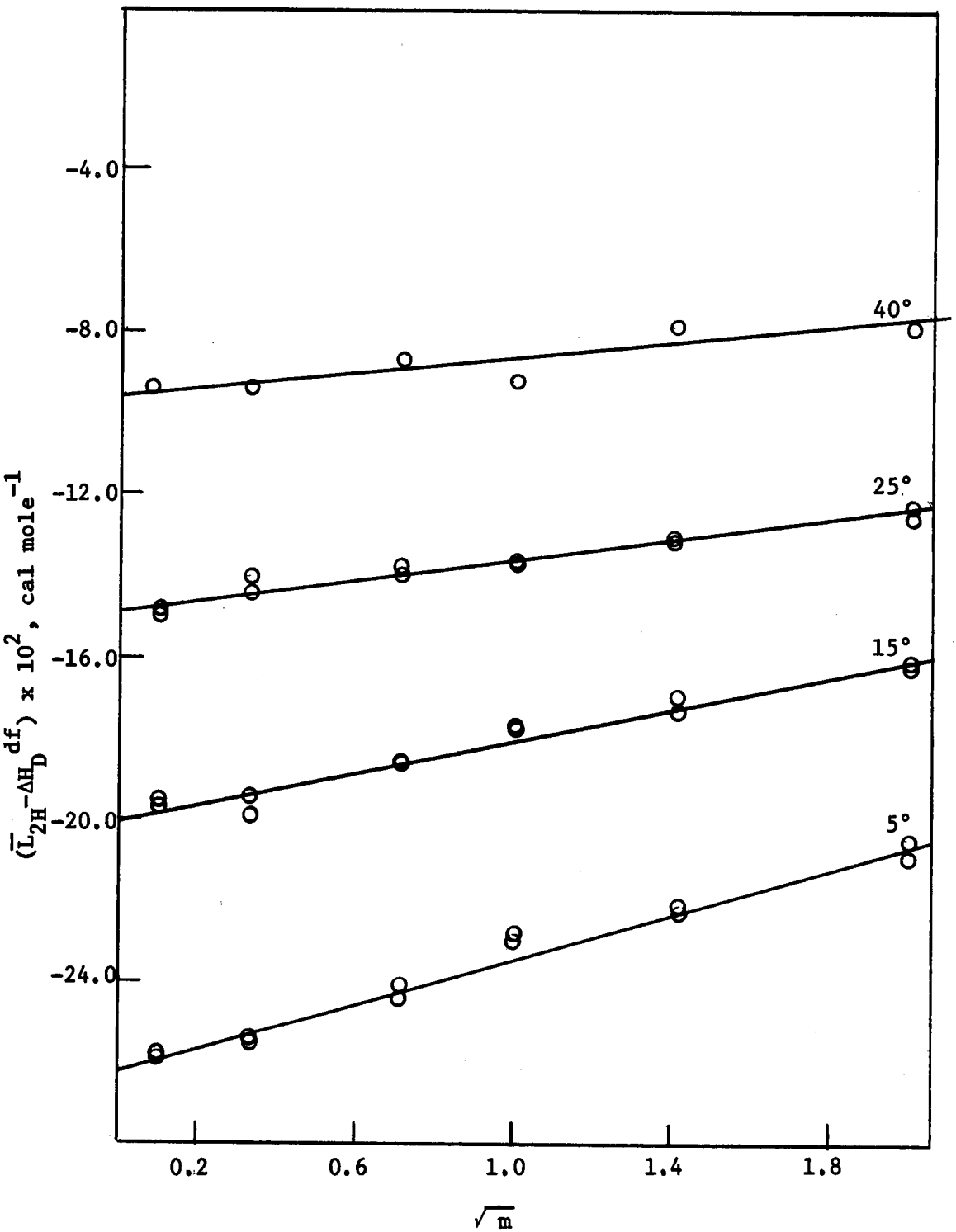

Figure 6. Plot of $(\bar{L}_{2H} - \Delta H_D^{df})$ vs. $\sqrt{m}$.

$$\bar{L}_2 = \bar{L}_{2H} - \bar{L}_{2D} = (d + eT)\sqrt{m} \quad . \qquad (21)$$

The temperature dependence and the precision of the isotope effect are such that no simple function (having a reasonable number of parameters) would describe the data over the full temperature range within experimental error. For this reason, it was decided to divide the data into two temperature ranges. The 5, 15, and 25° data were fit to Equation 20 and the following parameters obtained:

$a = -6.250009 \times 10^4 \pm 7.4839 \times 10^3$,

$b = 3.62985 \times 10^2 \pm 5.1917 \times 10^1$, $c = -5.30983 \times 10^{-1} \pm 9.0000 \times 10^{-2}$,

$d = 2.49471 \times 10^3 \pm 2.3921 \times 10^2$, and

$e = -7.96725 \times 10^0 \pm 8.2834 \times 10^{-1}$.

The variance of fit was 6.37×10^2. The 25 and 40° data were then fit to Equation 20. The variance of fit was 7.30×10^2 and the parameters are:

$a = -1.19165 \times 10^4 \pm 4.7886 \times 10^2$,

$b = 3.50049 \times 10^1 \pm 1.5792 \times 10^0$, $c = 0.0$,

$d = 6.52740 \times 10^2 \pm 4.21993 \times 10^2$,

and $e = -1.78221 \times 10^0 \pm 1.39179 \times 10^0$.

Values of $\Delta\bar{L}_2$ can be calculated using Equation 21. An equation giving the isotope effect on $\bar{L}_1$, $\Delta\bar{L}_1$, can be obtained by performing a Gibbs-Duhem integration.

$$\Delta\bar{L}_1 = \bar{L}_{1H} - \bar{L}_{1D} = -\frac{(d + eT)\, m^{3/2}}{(3)(55.508)} \qquad (22)$$

Values of $\Delta\bar{L}_2$ and $\Delta\bar{L}_1$ at rounded temperatures and concentrations are presented in Appendix II. Values of $\bar{L}_{1D}$ can be calculated from Equation 22 using $\bar{L}_{1H}$ from Equation 19 (p 37).

5. Fit of $\bar{L}_{2H}-\Delta H_D^{df}$ to the Extended Debye-Hückel Equation

It is of interest to see if the isotope effect on $\bar{L}_2$ can be described with one or more forms of the extended Debye-Hückel equation. An equation for the isotope effect on $\bar{L}_2$ can be obtained by writing separate equations (Equation 14, p 28) for NaCl in H_2O and D_2O and then subtracting. Since experimental values of $\bar{L}_{2D}$ are not known, it is necessary to modify the expression for $\bar{L}_{2H}-\bar{L}_{2D}$ by adding L_{2D}^s in the parametric form $(a + bT + cT^2)$. The resulting equation is given by

$$\bar{L}_{2H}-\Delta H_D^{df} = \nu RT^2 [(DH_H-DH_D) + \Delta BI + \Delta CI^2 + ---] + (a + bT + cT^2) \quad (23)$$

where DH_H and DH_D are the theoretical Debye-Hückel terms for H_2O and D_2O, respectively.

$$\Delta B = \frac{dB_H}{dT} - B_H\alpha_H - \frac{dB_D}{dT} + B_D\alpha_D \quad (24)$$

and

$$\Delta C = \frac{dC_H}{dT} - C_H\alpha_H - \frac{dC_D}{dT} + C_D\alpha_D \quad . \quad (25)$$

α is the coefficient of thermal expansion. B and C are assumed to have the temperature dependence

$$\Delta B = -\frac{\Delta B_1}{T^2} + \frac{\Delta B_2}{T} + \Delta B_3 \quad . \quad (26)$$

The following fits were performed using all the heat data and then using only the 5, 15, and 25° data because this was the range into which the data were broken for the empirical fit. The results of the fits are essentially the same. For this reason only the parameters for the fits to the 5, 15, and 25° data will be reported since these furnish a direct comparison with the empirical fit.

Although the concentration dependence of DH_H and DH_D is complicated, each has a term which contains $\sqrt{m}$ as a factor. Since the empirical fit (Equation 20, p 38) of $\bar{L}_{2H}-\Delta H_D^{df}$ shows a $\sqrt{m}$ dependence, it is reasonable to see if the observed isotope effect $(\bar{L}_{2H}-\Delta H_D^{df})$ can be accounted for by the isotope effects on the density of the solution, the dielectric constant, and the a° parameter which are all contained in the DH terms. Therefore, the experimental data were least-squared using only the DH terms with a°_D and $(\partial \ln a^\circ_D/\partial T)$ as the only adjustable parameters. The value of a°_H was fixed at 4.2 A° from activity coefficient data, and $(\partial \ln a^\circ_H/\partial T)$ was given the value of $-6.7 \times 10^{-6} {}^\circ K^{-1}$ found from the fit of $\bar{L}_{2H}$ (p 37).. The resulting fit is not good with a variance of fit of 3.54×10^3. The derived parameters are: $a^\circ_D = 2.17$ A° and $(\partial \ln a^\circ_D/\partial T) = 2.7 \times 10^{-3} {}^\circ K^{-1}$ which is more than a thousand times larger and of opposite sign to $(\partial \ln a^\circ_H/\partial T)$. The value of a°_D is not in the range expected. If the a° parameter is given the physical interpretation of the distance of closest approach of two ions in solution, then it is reasonable to bound the isotope effect $\Delta a^\circ/a^\circ_H = (a^\circ_H - a^\circ_D)/a^\circ_H$ between limits defined by the molar volume isotope effect[33] (MVIE), $\Delta V/V_H$ (or $\Delta V/3V_H$), on the one hand, and the isotope effect on the mean square amplitude[42] of an O-H versus and O-D stretch in water on the other. The molar volume isotope effect is a bulk phase approximation while the isotope effect on the mean square amplitude is an isolated molecule approximation. In this fashion one places generous lower and upper limits on $\Delta a^\circ/a^\circ_H$ of about -0.005 and +0.005, respectively. Thus, the fit using only the DH terms indicates that the $\sqrt{m}$

dependence can not originate solely from this term and that a°_D and $(\partial \ln a^\circ_D/\partial T)$ derived from the fit are not physically realistic. The bulk of the isotope effect must come from another source.

The data were refit with the addition of the first empirical term (ΔB_3 was set equal to zero) and with $(\partial \ln a^\circ_D/\partial T)$ and $(\partial \ln a^\circ_H/\partial T)$ set equal to zero. The variance of fit was 1.26×10^3 and $a_D^\circ = 16.9$ A°. The addition of the second empirical term gave a variance of fit of 6.53×10^2 and $a^\circ_D = 10.4$ A°. It is obvious that a reasonable value of a°_D can not be obtained from fits to the extended Debye-Hückel equation. Accordingly, the isotope effect on a° was restricted to (a still unreasonable) 5%, and the data were refit using the first two empirical terms. As expected, the variance of fit (9.34×10^2) increased. As a further test of the significance of the DH terms, they were set equal to zero and only the first two empirical terms were used. The fit without the DH terms is slightly better (variance of fit = 8.82×10^2) than that in which the isotope effect on a° was fixed at 5%. This indicates that the contribution of the DH terms to the isotope effect on $\bar{L}_{2H}-\Delta H_D^{df}$ is not significant.

It is important to note that a fit to any form of the extended Debye-Hückel equation requires at least three more parameters to describe the data as well as the empirical fit (Equation 20, p 38) to the $\sqrt{m}$ function.

6. Heats of Dilution

The isotope effect on heats of dilution can be used in a comparison with the effects calculated from Equations 21 and 22 (p 42).

Experimental values of the heat of dilution in H_2O, ΔH_H^{dil}, and D_2O, ΔH_D^{dil}, along with the isotope effect are given in Table V. (Isotope effects on heats of dilution of KCl are given in Appendix III.)

The quantity $\Delta\bar{L}_1$ can be used as a link between the dilution and the differential heat measurements. Values of $\Delta\bar{L}_1$, can be calculated from the isotope effect on the heats of dilution by[43]

$$\Delta\bar{L}_1 = -\frac{m^2}{55.508}\left(\frac{\partial\Delta\phi L_2}{\partial m}\right) . \qquad (27)$$

In Equation 27, $\Delta\phi L_2$ is the isotope effect on the relative apparent molal enthalpy which can be written as

$$\Delta\phi L_2 = \Delta\phi H_2 - \Delta\phi H_2^{\circ} \qquad (28)$$

where $\Delta\phi H_2$ is the isotope effect on the apparent molal enthalpy at some concentration, m, and $\Delta\phi H_2^{\circ}$ is the isotope effect on the apparent molal enthalpy at infinite dilution. From Equation 27, the slope of $\Delta\phi L_2$ with respect to m is needed to calculate $\Delta\bar{L}_1$, but from Equation 28 it can be seen that

$$\left(\frac{\partial\Delta\phi L_2}{\partial m}\right) = \left(\frac{\partial\Delta\phi H_2}{\partial m}\right) \qquad (29)$$

since $\Delta\phi H_2^{\circ}$ is not a function of the concentration. Thus,

$$\Delta\bar{L}_1 = -\frac{m^2}{55.508}\left(\frac{\partial\Delta\phi H_2}{\partial m}\right) . \qquad (30)$$

Assuming the concentration dependence of Equation 22 (p 42) (found from differential heats) to be valid, Equation 31 can be derived by combining Equations 22 and 30.

$$\Delta\phi H_2 = \frac{2(d + eT)\sqrt{m}}{3} \qquad (31)$$

Thus, the concentration dependence found for the differential heat of

TABLE V

HEATS[a] OF DILUTION (ΔH^{dil}) IN H_2O AND D_2O

t, °C	m_i	m_f	ΔH_H^{dil}	ΔH_D^{dil}	$\Delta H_H^{dil} - \Delta H_D^{dil}$
10	3.40	0.155	765 ± 1	953 ± 7	-188 ± 8
25	3.40	0.155	423 ± 1	530 ± 3	-107 ± 4
	5.50	0.230	568 ± 11	683 ± 10	-115 ± 15
50	3.40	0.155	22 ± 2	66 ± 1	-44 ± 2
	5.50	0.230	33 ± 2	84 ± 3	-51 ± 4
75	3.40	0.155	-280 ± 14	-279 ± 16	-1 ± 21
	5.50	0.230	-433 ± 11	-393 ± 5	-40 ± 12

[a]Units are cal $mole^{-1}$.

solution data predicts that a plot of $\Delta\phi H_2$ versus $\sqrt{m}$ is a straight line and that the slope, S_A, is given by

$$S_A = \frac{2(d + eT)}{3} \tag{32}$$

The corresponding slope, S_B, from the heat of dilution is given by

$$S_B = \frac{\Delta\phi H_2(m_i) - \Delta\phi H_2(m_f)}{\sqrt{m_i} - \sqrt{m_f}} \tag{33}$$

The numerator is the negative of the isotope effect on the heat of dilution from concentration m_i to m_f.

Values of the slopes calculated from these isotope effects on heats of dilution together with those obtained from the differential heat of solution measurements via Equation 32 are given in Table VI (with error estimates) and are compared to slopes calculated from the available literature data[44,45] on the dilution isotope effect. All these different data are in satisfactory agreement.

Some additional comments on the comparisons implicit in Table VI are in order. Wood[44] originally chose to describe his dilution isotope effect data (25°) at 1,2, and 3 m by fitting to the form

$$\Delta\phi L_2 = k_1 m + k_2 m^2 \tag{34}$$

thus obtaining $k_1 = 53.6$ cal mole^{-1} m^{-1} and $k_2 = -7.1$ cal mole^{-1} m^{-2}. Other authors[9,10,44-46] have also assumed an m or m + m^2 concentration dependence for isotope effects. The present demonstration that the isotope effect is proportional to $\sqrt{m}$ is only possible because the data extend over a wider range and to low concentration (0.01 to 4 m). This results in an important difference when calculated thermodynamic properties are compared with those obtained from the assumed m or m + m^2

TABLE VI

SLOPES[a] OF $\Delta\phi H_2$ WITH RESPECT TO $\sqrt{m}$

Reference	t, °C	m_i	m_f	S_A (Equation 32)	S_B (Equation 33)
A[b]	10	3.40	0.155	159 ± 11	130 ± 5
A	25	3.40	0.155	80 ± 6	74 ± 3
A		5.50	0.230		62 ± 8
44		3.00	0.390		78 ± 4
44		2.00	0.267		71 ± 4
44		1.00	0.138		64 ± 4
45		2.95	0.0		59 ± 7
A	50	3.40	0.155	51[c]	30 ± 4
A		5.50	0.230		27 ± 3
A	75	3.40	0.155	32[c]	1 ± 14
A		5.50	0.230		2 ± 1

[a]Units are in cal $mole^{-1}$ $m^{-1/2}$.

[b]Present work.

[c]Calculated by extrapolation from 40°.

functions of other authors. The difference is significant because much thermodynamic information is sensitive to the functional relation used to extrapolate the data to infinite dilution. Although all the relations agree at the origin (because of the definition of relative properties) and at higher concentrations ($\sim$ 2 or 3 m), the difference between the functional form of m ($m + m^2$ also reduces to m at lower concentrations) and $\sqrt{m}$ is not small for concentrations between 0 and 1 or 2 m. An example of the magnitude of this difference is given in the next section (p 54).

7. Integral Heats

Integral heats of solution which result in a low final concentration can be used to approximate L_2^s (p 33). An exact representation of the experimental heat, q^I, resulting from an integral heat measurement is given by

$$q^I = n_1\bar{L}_1 + n_2\bar{L}_2 - n_2L_2^s \tag{35}$$

where n_1 and n_2 are the moles of solvent and solute, respectively. Thus, the measured heat is equal to the heat from the solution of n_2 moles of salt at infinite dilution, $-n_2L_2^s$, plus the negative of the heat of dilution from the final concentration to infinite dilution, $n_1\bar{L}_1 + n_2\bar{L}_2$. Equation 35 can be written on a per mole of salt basis as

$$\Delta H^I = \frac{n_1}{n_2}\,\bar{L}_1 + \bar{L}_2 - L_2^s \tag{36}$$

where ΔH^I is the integral heat of solution per mole of salt added. The isotope effect on the integral heat of solution, $\Delta H_H^I - \Delta H_D^I$, is

$$\Delta H_H^I - \Delta H_D^I = \frac{n_1}{n_2}\,\Delta\bar{L}_1 + \Delta\bar{L}_2 - \Delta L_2^s \tag{37}$$

On the molality scale $n_2 = m$ and $n_1 = 55.508$. Values of the integral heat of solution of NaCl in H_2O, ΔH_H^I, and D_2O, ΔH_D^I, and the isotope effect are given in Table VII. (Integral heat data for other salts are given in Appendix III.) Values of ΔL_2^s can be calculated from Equation 37 (Method 1) using $\Delta\bar{L}_2$ from Equation 21 (p 42) and $\Delta\bar{L}_1$ from Equation 22 (p 42). Also the quantity $(a + bT + cT^2)$ from Equation 20 (p 38) is equal to L_{2D}^s, and ΔL_2^s can be calculated (Method 2)

$$\Delta L_2^s = L_{2H}^s - (a + bT + cT^2) \qquad (38)$$

where values of L_2H^s are taken from the data of Criss and Cobble.[35] Table VIII contains values of ΔL_2^s calculated by using Methods 1 and 2. Also included in Table VIII are values of ΔL_2^s calculated by Method 1 using the isotope effects on the integral heat of solution which are available from the literature.[46-48] At 25° the values of ΔL_2^s calculated from the data of different investigators are in excellent agreement. The values of ΔL_2^s calculated by Method 2 are in reasonable agreement with those of Method 1, but the values of ΔL_2^s calculated from the isotope effect on the integral heats of solution (Method 1) are judged to be the more reliable because they are more directly determined (relatively small correction to give ΔL_2^s).

Desnoyers[46] measured the isotope effect on the integral heat of solution and on the heat of dilution. He fit his dilution data to Equation 34 (p 48) and the values of k_1 and k_2 are in agreement with those found by Wood.[44] However, Desnoyers does not report the dilution data or the concentrations except to state that the concentrations were less than 3 m. He then uses the isotope effect on the heat of dilution (calculated from Equation 34) from concentration m to infinite dilution

TABLE VII

INTEGRAL HEATS OF SOLUTION (ΔH^I)[a,b] OF NaCl IN H_2O AND D_2O

t, °C	ΔH_H^I	ΔH_D^I	$\Delta H_H^I - \Delta H_D^I$
5	1593 ± 31	2390 ± 34	-797 ± 46
10	1412 ± 17	2114 ± 23	-702 ± 29
25	979 ± 7	1515 ± 9	-536 ± 12
50	411 ± 3	756 ± 3	-345 ± 5
75	-101 ± 6	148 ± 4	-249 ± 8

[a] Units are cal $mole^{-1}$.

[b] Final concentration of solution was 0.465 m.

TABLE VIII

VALUES OF ΔL_2^{s} [a] FOR NaCl

Reference	t, °C	m	$\Delta H_H^I - \Delta H_D^I$	ΔL_2^s (Method 1)	ΔL_2^s (Method 2)
A[b]	5	0.465	-797 ± 46	924 ± 47	959 ± 17
A	10	0.465	-702 ± 29	811 ± 30	853 ± 15
A	25	0.465	-536 ± 12	590 ± 13	566 ± 10
47		0.250	-545 ± 3	585 ± 5	
47		0.500	-524 ± 1	580 ± 3	
46		0.500	-523[d]	579	
48		0.250	-560[d]	599	
A	50	0.465	-345 ± 5	364[c]	
A	75	0.465	-249 ± 8	250[c]	

[a] Units are cal $mole^{-1}$.

[b] Present work.

[c] $\Delta\bar{L}_1$ and $\Delta\bar{L}_2$ were calculated from dilution data of Table V, p 47.

[d] Errors not given by authors.

to calculate ΔL_2^s from the isotope effect on the integral heat of solution at m'. For example, using his value of the isotope effect on the integral heat of solution of -523 cal mole^{-1} at 0.5 m, Desnoyers calculates 548 cal mole^{-1} for ΔL_2^s. This compares to 579 cal mole^{-1} (Table VIII) calculated using Equation 37 (p 50) and the $\sqrt{m}$ concentration dependence (to give $\Delta\bar{L}_1$ and $\Delta\bar{L}_2$) of the present work. Obviously both curves (for the correction to infinite dilution) agree at m = 0 by virtue of the definition of $\Delta\bar{L}$ and $\Delta\phi_L$ as relative quantities. They also agree at high concentrations ($\sim$ 2 to 3 m) where the two sets of data overlap. Therefore, significant differences are found in the region between 0 and 1 or 2 m, and it is these which account for the different (31 cal mole^{-1}) corrections. The example illustrates again the great importance of proper functional forms for the extrapolation to infinite dilution.

8. Heat Capacities

Values of ΔL_2^s were determined in the previous section (p 51) by two methods (1 and 2). It follows that

$$-\left(\frac{d\ \Delta L_2^S}{dT}\right) = \phi_{c(H)}^{\circ} - \phi_{c(D)}^{\circ} = \Delta\phi_c^{\circ} \qquad (39)$$

where ϕ_c° is the apparent molal heat capacity at infinite dilution which is also the standard partial molal heat capacity, $\bar{C}_p^{\circ}$. Values of $(d\ \Delta L_2^s/dT)$ were determined graphically from smooth curves drawn through values of ΔL_2^s plotted versus the temperature. The resulting heat capacities are given in Table IX. The values of 12 (Method 1) and 10 (Method 2) cal°K^{-1} mole^{-1} at 25° compare very favorably with 9.6 cal°K^{-1} mole^{-1} reported by Fortier, Philip and Desnoyers[49].

TABLE IX

VALUES OF $\Delta\overline{C}_p^{\circ}$[a] ($\Delta\phi_c^{\circ}$) FROM ΔL_2^s

t, °C	$\Delta\overline{C}_p^{\circ}$ (Method 1)	$\Delta\overline{C}_p^{\circ}$ (Method 2)
5	25	21
10	22	21
25	12	10
50	6	
75	3	

[a]Units are cal $°K^{-1}$ $mole^{-1}$.

who made direct measurements of the apparent molal heat capacities.

A further comparison can be made by calculating the isotope effect on $\bar{J}_2$ which is the relative partial molal heat capacity of the salt (solute) and can be expressed as

$$\bar{J}_2 = \left(\frac{\partial L_2}{\partial T}\right). \tag{40}$$

The isotope effect, $\Delta\bar{J}_2$, is given by

$$\Delta\bar{J}_2 = \left(\frac{\partial L_{2H}}{\partial T}\right) - \left(\frac{\partial L_{2D}}{\partial T}\right) = \left(\frac{\partial \Delta L_2}{\partial T}\right). \tag{41}$$

Therefore, values of $\Delta\bar{J}_2$ can be calculated from the isotope effect on $\bar{L}_2$ determined from differential heats of solution. The slope $(d\Delta L_2/dT)$ was obtained graphically from a smooth curve drawn through values of $\Delta\bar{L}_2$ at 1 m. The resulting slope gives $\Delta\bar{J}_2 = -5$ cal $°K^{-1}$ $mole^{-1}$.

$\bar{J}_2$ can be ascertained from Desnoyers' data by[50]

$$\bar{J}_2 = \phi_c - \phi_c° + 1/2\ m^{1/2} \left(\frac{d\phi c}{dm^{1/2}}\right). \tag{42}$$

Using Desnoyers' fit of the apparent molal heat capacity, values of $\bar{J}_{2H}$ and $\bar{J}_{2D}$ were calculated. The isotope effect, $\Delta\bar{J}_2$, is simply

$$\Delta\bar{J}_2 = \bar{J}_{2H} - \bar{J}_{2D} \quad . \tag{43}$$

At 1 molal $\Delta\bar{J}_2$ is equal to -4.0 cal$°K^{-1}$ which is in excellent agreement with the value of -5 cal$°K^{-1}$ $mole^{-1}$ from the differential heats of solution. The agreement with directly measured heat capacities is gratifying because the calculation of heat capacities from measured enthalpies is a stringent test of the data.

C. Osmotic Coefficient Data from the Measurement of Freezing Point Depressions

1. Thermodynamics

In using measurements of freezing point depressions to determine solvent activities or osmotic coefficients, it is necessary to correct the data to a standard temperature since each measurement is made at a different temperature (the freezing point of the solution). Normally the freezing point of the pure solvent is chosen as the standard temperature. The equilibrium between the liquid solvent (in solution) and pure solid solvent is the process of concern in freezing point measurements. Equation 44 expresses the relation between the temperature dependence of the activity of the solvent, a_1, and the heat of fusion, ΔH_f°, of the pure solvent.

$$\left(\frac{\partial \ln a_1}{\partial T}\right)_p = \frac{\Delta H_f^\circ}{RT^2} \tag{44}$$

It must be recognized that ΔH_f° is a function of temperature,

$$\left(\frac{\partial \Delta H_f^\circ}{\partial T}\right) = \Delta C_p \ . \tag{45}$$

(ΔC_p is the difference between the heat capacity of the pure ice and pure supercooled solvent.) It is customary to express ΔC_p with a power series.

$$\Delta C_p = \Gamma_0 + \Gamma_1 t + \Gamma_2 t^2 + \text{---} \tag{46}$$

Γ_0, Γ_1, and Γ_2 are parameters determined from experiment. Integration of Equation 46 followed by substitution into Equation 44 gives an equation which can now be integrated to yield the activity a_1.

$$\ln a_1 = A_1\theta + \frac{B_1\theta^2}{2} + \frac{C_1\theta^3}{3} + \frac{D_1\theta^4}{4} \qquad (47)$$

where:

$$A_1 = \frac{\Delta H_f^\circ}{RT_f^2}, \quad B_1 = \frac{2\Delta H_f^\circ}{RT_f^3} - \frac{\Gamma_o}{RT_f^2},$$

$$C_1 = \frac{3\Delta H_f^\circ}{RT_f^4} - \frac{2\Gamma_o}{RT_f^3} + \frac{\Gamma_1}{2RT_f^2}, \quad \text{and}$$

$$D_1 = \frac{4\Delta H_f^\circ}{RT_f^5} - \frac{3\Gamma_o}{RT_f^4} + \frac{\Gamma_1}{RT_f^3} - \frac{\Gamma_2}{3RT_f^2}.$$

In Equation 47 and in the definition of the terms following, θ is the freezing point depression, T_f(°K) is the freezing point of the pure solvent, and ΔH_f° is the heat of fusion of the pure solvent at its freezing point, T_f. Equation 47 gives an expression for the activity of the solvent at the freezing point of the solution. The activity of the solvent at any other temperature can be obtained by the use of Equation 48.

$$\left(\frac{\partial \ln a_1}{\partial T}\right)_{p,m} = \frac{-\bar{L}_1}{RT^2} \qquad (48)$$

where $\bar{L}_1$ is the relative partial molal enthalpy of the solvent and is a function of the temperature and concentration.

The integration of Equation 48 from the freezing point of the solution to the freezing point of the solvent allows calculation of the solvent activity at the standard temperature from the observed value at the freezing point of the solution.

The practical osmotic coefficient of the solvent, ϕ, is defined in terms of the solvent activity by

$$\phi = - \frac{\ln a_1 \ (55.508)}{\nu m} . \qquad (49)$$

The osmotic coefficient has an advantage over the activity in that it is a more sensitive measure of the deviation from ideality.

2. H_2O Data

The measured freezing point depressions for NaCl in H_2O are given in Table X. Other freezing point data for NaCl in H_2O have been reported by Scatchard and Prentiss,[21] Momicchioli, Devoto, and Cocco,[51] and most recently by Gibbard and Gossmann.[52] Osmotic coefficients for all these data and for the data of the present work were calculated at 0° by the use of Equations 47, 48 (p 58) and 49 and the fit of $\overline{L}_{1H}$ data given by Equation 19 (p 37). Osborne's[53] value of -1436 $\pm$ 1 cal $mole^{-1}$ was used for the heat of fusion of pure water. The heat capacities of Osborne, Stimson, and Ginnings[54] for liquid H_2O between 0 and 10° and of Dickinson and Osborne[55] for H_2O ice between -2 and -30° were smoothed by least-squares to relations of the type

$$C_p = a_0 + a_1 t + a_2 t^2 \ . \qquad (50)$$

The equations form good representations of the data and the fits are within experimental error. Since the heat capacity data for liquid H_2O do not extend into the supercooled region, it was necessary to use the smoothed function determined for C_p of liquid H_2O above 0° to extrapolate below the freezing point. The values of ΔC_p were then fit to Equation 46 (p 57) and the values of the parameters found:

TABLE X

FREEZING POINT DEPRESSIONS IN H_2O

m	θ
0.0068007	0.02453
0.015864	0.05674
0.019826	0.07004
0.027412	0.09705
0.040817	0.14375
0.042750	0.14980
0.045616	0.15963
0.048375	0.16932
0.055046	0.19278
0.066782	0.23263
0.083026	0.28734
0.086649	0.30087
0.093923	0.32526
0.10641	0.36771
0.14145	0.48704
0.19614	0.67024
0.20380	0.69645
0.25884	0.88191
0.26676	0.90771
0.32913	1.11666
0.37877	1.28604
0.45792	1.54809
0.49602	1.67554
0.65089	2.19585
0.72042	2.43116
0.86203	2.91251
0.90633	3.05690
1.0239	3.45997
1.2366	4.19669

TABLE X (Continued)

m	θ
1.4940	5.10716
1.8218	6.29583
4.1928	16.21277

$$\Gamma_0 = -9.02280 \pm 7.3 \times 10^{-4} \text{ cal mole}^{-1} \text{ deg}^{-1}$$

$$\Gamma_1 = 5.37240 \times 10^{-2} \pm 6.6 \times 10^{-6} \text{ cal mole}^{-1} \text{ deg}^{-2}$$

and $$\Gamma_2 = -3.48631 \times 10^{-4} \pm 5.7 \times 10^{-8} \text{ cal mole}^{-1} \text{ deg}^{-3} \quad .$$

3. Fitting of ϕ_H (0°) from All Freezing Point Data and Discussion of Errors

The osmotic coefficients at 0° from all the freezing point data were then least-squared to Equation 12 (p 28). In this fitting process an initial trial with all points weighted equally allowed us to calculate a deviation function and an associated error band for each set of data. Each point was then weighted as $1/\sigma^2$ where σ was taken as half the smoothed error band. (Weights for the data points varied from 0.03 to 1.0 with most of the points assigned weights close to one. Only a few obviously deviant points were weighted as low as 0.03.) A deviation plot from this new function was again calculated and is shown in Figure 7. It is apparent from the plot that the internal consistency of the Scatchard-Prentiss data is superior, and it was therefore assigned a slightly higher weight than the present data or that from the other laboratories. (On the average $(1/\sigma^2)_{sp} \approx 1.2\ (1/\sigma^2)$ present.) On the other hand, their accuracy is no better than that of the present work. The parametric values of the fit based on Equation 12 are as follows:

$$a_H^\circ = 4.45091 \times 10^{-8} \pm 4.797 \times 10^{-10},$$

$$B = -1.03255 \times 10^{-2} \pm 1.7630 \times 10^{-3},$$

$$C = 2.12593 \times 10^{-2} \pm 8.797 \times 10^{-4}, \text{ and}$$

$$D = -2.15460 \times 10^{-3} \pm 1.3572 \times 10^{-4} \quad .$$

The variance of fit was 1.33×10^{-6} and indicates that osmotic coefficients

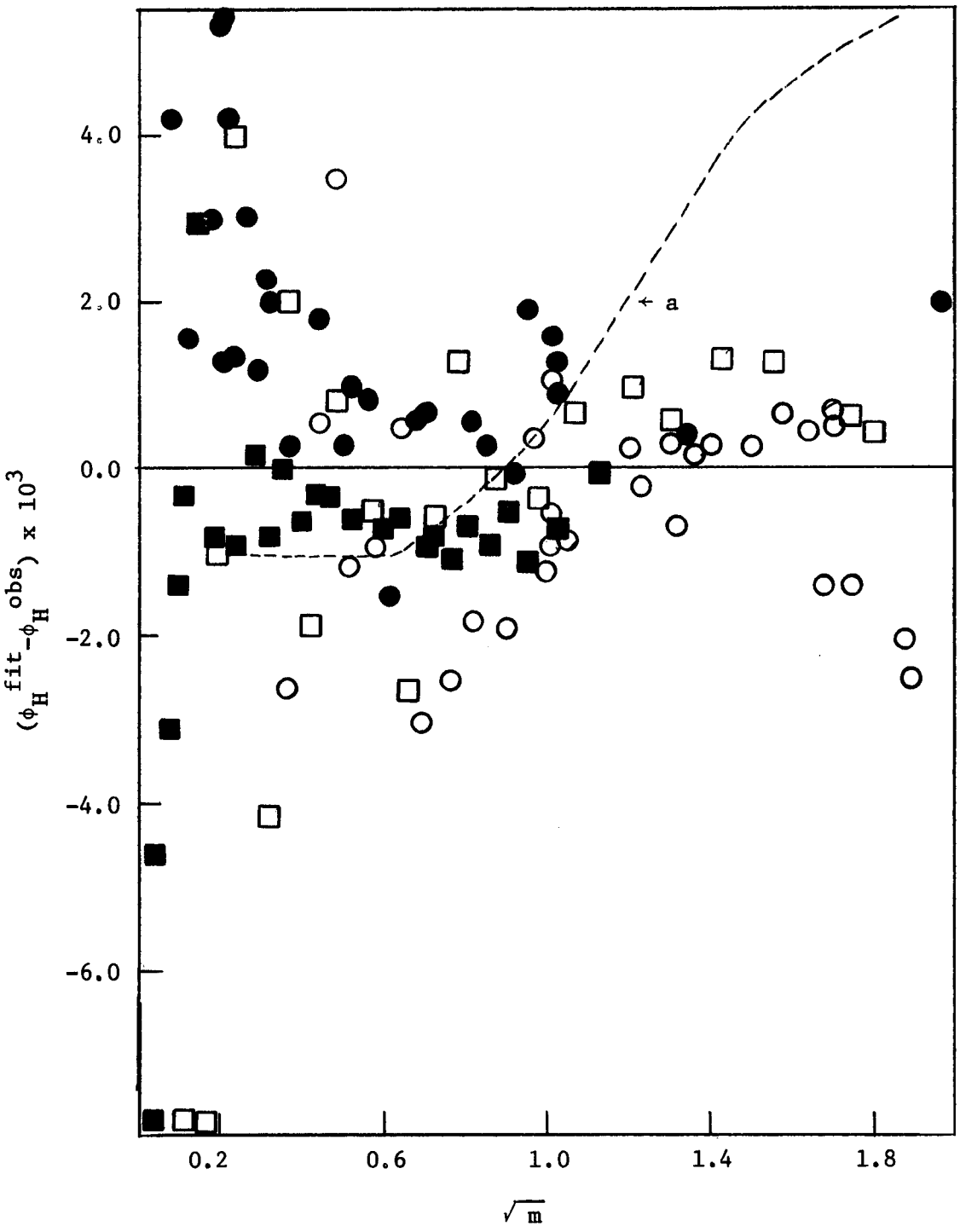

Figure 7. Deviation plot for all freezing point data.

Closed circles: present work; closed squares: Scatchard and Prentiss;[21] open circles: Gibbard and coworkers;[52] open squares: Momicchioli and coworkers;[51] Line a: fit of Gibbard and coworkers.[56]

from freezing points (the method of choice for dilute solutions) are known to no better than $\pm$ 0.001 unit at any concentration.

Gibbard, Scatchard, Rousseau, and Creek[56] (GSRC) have recently fit osmotic coefficient data for H_2O solutions of NaCl to an equation similar to our Equation 12 (p 28). They included data from different laboratories as determined by both freezing points (at the freezing point of the solution) and vapor pressure measurements (above 298°K). Figure 7 includes a line labeled "a" which shows the deviation of the GSRC fit from that reported above for the available freezing point data corrected to 0°. The two agree well at lower concentrations. They are within 0.001 unit to $\sim$ 1 m. The deviation however increases with concentration reaching as much as $\sim$ 0.006 at 3 m. The deviation of the GSRC fit at 25° from the freezing point data as corrected (Equation 48, p 58) to 25° is similar to 0° behavior (Figure 7, p 63). It again increases with concentration to as much as $\sim$ 0.009 at 3 m. GSRC agrees well ($\pm$ 0.001) with Platford's[57] isopiestic measurements at 0° and with the well accepted Robinson and Stokes'[58] data at 25°. Since the difference at 25° is not substantially greater than that at 0°, it appears that most of the differences with the freezing point data result from the process of correcting the data from the freezing point of the solution to 0°. The correction to 0° for the most concentrated solutions ($\sim$ 4 m) involves an integration of $(-\bar{L}_{1H}/RT^2)dT$ from $\sim$ -15 to 0°, while the correction to 25° requires an additional integration from 0 to 25°. The values of $\bar{L}_{1H}$ below 5° are calculated by an extrapolation of the $\bar{L}_{1H}$ data (at 5, 15, 25, and 40°). As the

concentration increases, the temperature at the freezing point of the solution decreases. This necessitates a longer and less precise extrapolation to determine the value of $\bar{L}_{1H}$. Also as the concentration increases, the value of $\bar{L}_{1H}$ increases, and this results in a larger correction. The combination of these two factors accounts for the error in the correction. For example, a 3 m NaCl solution (H_2O) freezes at $\sim$ -11° and the extrapolated value of $\bar{L}_{1H}$ is 51.7 cal mole^{-1}. By making a reasonable estimate of the error in the extrapolation of $\bar{L}_{1H}$ to -11°, the error involved in calculating the osmotic coefficient at 0° from that at -11° can be determined and is equal to 0.005 osmotic coefficients units. This is approximately the amount by which the osmotic coefficient calculated from freezing point data differ from Gibbard's fit at 0° and 3 m. Additionally, it should be noted that Young[59] extrapolated his values of $\bar{L}_{1H}$ (measured at 0, 12.5, and 25°) to the freezing point of NaCl solutions (up to $\sim$ 5 m) and that his values agree well with those used in the present work. The corrections to 25° from 0° does not involve a long extrapolation of the $\bar{L}_{1H}$ data, and the correction becomes relatively smaller since $\bar{L}_{1H}$ decreases with increasing temperature. Accordingly, it is reasonable that almost all of the error in the integration be assigned to the interval between the freezing points of the more concentrated solutions and 0°.

4. D_2O Data

Although the freezing point depressions of the NaCl solutions in D_2O were measured in a straightforward and analogous fashion to those in H_2O, it will generally be useful to express the results in terms of

isotopic differences from the H_2O data at the same concentration. To that end, it is appropriate to derive smoothed values of the freezing point depressions in H_2O, θ_H, so that values of $\Delta\theta = \theta_H - \theta_D$ can be calculated from the combination of each D_2O data point with a smoothed value for H_2O. The procedure for the smoothing process is a modification of one first used by Scatchard.[14] An approximate expression for the osmotic coefficient in terms of the freezing point depression is given by

$$\phi = \frac{\theta}{\nu\lambda m} \quad . \tag{51}$$

Here λ is the molal freezing point constant for the solvent and is given by

$$\lambda = \frac{RT_f^2}{\Delta H_f^\circ (55.508)} \quad . \tag{52}$$

ΔH_f° is the heat of fusion of the pure solvent at its freezing point, T_f. Lietzke[30] has fit osmotic coefficients of H_2O as a function of temperature and NaCl concentration. His equation was used to calculate values of the osmotic coefficient at the concentration and temperature of the freezing point measurements which were then subtracted from the osmotic coefficients calculated by Equation 51. The differences were then least-squared to a deviation function ($\phi_{Eq\ 51} - \phi_{Lietzke} = -6.998 \times 10^{-3} \sqrt{m} - 4.115 \times 10^{-3}$). Smoothed values of the osmotic coefficient at any concentration can be calculated by adding the smoothed differences calculated from the fit to the values predicted by Lietzke's equation. A smooth value of θ_H was calculated (Equation 51) for each NaCl concentration at which freezing point measurements were made in D_2O.

Each freezing point depression in D_2O, θ_D, was corrected for H_2O contamination

$$(\theta_H - \theta_D)_{correct} = \frac{(\theta_H - \theta_D)_{measured}}{X_{D_2O}} \qquad (53)$$

where X_{D_2O} is the mole fraction of D_2O (X_{D_2O} was never smaller than 0.992). Thus, the corrected value of θ_D is given by

$$\theta_D = -(\theta_H - \theta_D)_{correct} + \theta_H. \qquad (54)$$

Values of θ_D corrected for H_2O contamination along with smoothed values of $(\theta_H)_s$ are presented in Table XI.

5. Heat of Fusion of D_2O: The Intercept

An expression for θ can be written for H_2O and D_2O solutions by the use of Equation 51 (p 66). These are then subtracted to give

$$\theta_H - \theta_D = \nu m (\lambda_H \phi_H - \lambda_D \phi_D) \quad . \qquad (55)$$

Following previous conventions, one can write $\Delta\phi = \phi_H - \phi_D$, $\Delta\lambda = \lambda_H - \lambda_D$, and $\Delta\theta = \theta_H - \theta_D$.

Equation 56 results after substitutions and rearrangement.

$$\frac{\Delta\theta}{\theta_H} = \frac{\nu m \lambda_D \Delta\phi}{\theta_H} + \frac{\Delta\lambda}{\lambda_H} \quad . \qquad (56)$$

Assuming $\Delta\phi = k_1 m + k_2 m^2$,

$$\frac{\Delta\theta}{\theta_H} = \frac{\nu m^2 \lambda_D (k_1 + k_2 m)}{\theta_H} + \frac{\Delta\lambda}{\lambda_H} \quad . \qquad (57)$$

A graph of $\Delta\theta/\theta_H$ versus m^2/θ_H gives an intercept related to the isotope effect on the heat of fusion. A least-squares fit gave the following: $\frac{\Delta\lambda}{\lambda_H} = 2.00885 \times 10^{-2} \pm 4.660 \times 10^{-4}$, $2\lambda_D k_1 = 2.62832 \times 10^{-2} \pm 4.0972 \times 10^{-3}$, and $2\lambda_D k_2 = -1.08384 \times 10^{-2} \pm 2.0194 \times 10^{-3}$. The

TABLE XI

FREEZING POINT DEPRESSIONS FOR NaCl IN D_2O

m	$(\theta_H)_s$	θ_D
0.039332	0.13840	0.13553
0.057984	0.20254	0.19814
0.069873	0.24328	0.23899
0.108782	0.37556	0.36743
0.14406	0.49493	0.48484
0.14921	0.51221	0.50156
0.24889	0.84751	0.82790
0.25275	0.86044	0.84099
0.36212	1.22710	1.20064
0.43472	1.47048	1.43484
0.46938	1.58675	1.54919
0.49515	1.67322	1.63242
0.65440	2.20885	2.15246
0.66660	2.25000	2.19382
0.78688	2.65656	2.59167
0.80043	2.70248	2.63772
0.865360	2.92287	2.84977
0.93302	3.15323	3.07960
1.0085	3.41135	3.32802
1.0962	3.71193	3.62173
1.1497	3.89625	3.80045
1.2824	4.35605	4.24742
1.5443	5.27557	5.14891
1.8253	6.28310	6.14088
2.1981	7.65622	7.48367
4.3350	--	16.3411

variance of fit was 1.12×10^{-6}. The calculated isotope effect on the heat of fusion is 71 ± 2 cal mole^{-1} (using -1436 ± 1 cal mole^{-1}[53] as the heat of fusion of H_2O). This compares with the best calorimetric value of 65 ± 4 cal mole^{-1} and the value of 61 ± 8 cal mole^{-1} calculated from the vapor pressure isotope effect.[9] The heat of fusion of D_2O determined from the freezing point measurements is -1507 ± 3 cal mole^{-1}. Other assumed concentration dependencies, e.g., $\Delta\phi = k_1' \sqrt{m} + k_2'm$ give the same intercept within the statistical error and hence identical heats of fusion for D_2O.

6. Isotope Effect on ϕ

Osmotic coefficients for D_2O were calculated at the freezing point of the solution and corrected to the freezing point of pure D_2O (3.82°) using the same procedures employed for H_2O. The value of -1507 ± 3 cal mole^{-1} determined in the previous section was used for the heat of fusion of D_2O. The heat capacity of liquid D_2O[62,63] and D_2O ice[60] were smoothed as before (p 59). The parameters from the fit are: $\Gamma_o = -9.67492 \pm 1.14 \times 10^{-3}$ cal mole^{-1} deg^{-1}, $\Gamma_1 = 7.02572 \times 10^{-2} \pm 1.22 \times 10^{-5}$ cal mole^{-1} deg^{-2}, $\Gamma_2 = -4.45839 \times 10^{-4} \pm 1.01 \times 10^{-7}$ cal mole^{-1} deg^{-3}.

To minimize the effects of possible systematic errors in the isotope effect, the osmotic coefficients for H_2O from the present work were smoothed and used instead of the general fit (p 62) of all the freezing point measurements. This was done by fitting the deviations of the present data (0°) from the general fit to a difference equation. The systematic differences from other authors are shown in Figure 7 (p 63) where it can be seen that the particular correction under

discussion is small. It is described by the empirical equation

$$\phi_{\text{(present work)}} - \phi_{\text{(general fit)}} = P_1 \sqrt{m} + P_2 (m + P_3)^2 + P_4 \quad (58)$$

with $P_1 = 1.21746 \times 10^{-2}$, $P_2 = 7.79127 \times 10^{-4}$, $P_3 = -5.46756 \times 10^{0}$, and $P_4 = -2.82772 \times 10^{-2}$. Smoothed values of the osmotic coefficients at 0° were then corrected to 3.82°. The values of ϕ_H, ϕ_D, and the isotope effect, $\Delta\phi$, are reported in Table XII. The accuracy of the highest concentration point (4.3345 m) is questionable. The freezing point of a 4.3 m solution is about ten degrees below the lowest temperature used in the thermistor calibration, and therefore while the 4.3 m point is reported in Table XII, it was excluded from the fitting of $\Delta\phi$.

7. The Fitting of $\Delta\phi$ as a Function of m

It is reasonable to expect that within experimental error the concentration dependencies of the isotope effects on the osmotic coefficients and the relative partial molal enthalpies should be consistent. Additionally it is reasonable to expect that the concentration dependence of the isotope effect on the osmotic coefficients should be consistent with some form of the extended Debye-Hückel theory, even though other forms might be equally plausible. In this context recall that although the theoretical expression for $\Delta\bar{L}_2$, Equation 23 (p 43), was extremely complicated, the observed isotope effects displayed a simple $\sqrt{m}$ concentration dependence within the experimental error. Similar behavior might be expected for the isotope effects on the osmotic coefficients. This can easily be seen with the help of the following argument. Taking

TABLE XII

ISOTOPE EFFECT ON THE OSMOTIC COEFFICIENT AT 3.82°C

m	ϕ_D	ϕ_H	$\Delta\phi$
0.039332	0.9454	0.9456	0.0002
0.057984	0.9376	0.9392	0.0016
0.069873	0.9385	0.9361	-0.0024
0.10878	0.9269	0.9289	0.0020
0.14406	0.9237	0.9245	0.0008
0.14921	0.9225	0.9240	0.0015
0.24889	0.9133	0.9172	0.0039
0.25275	0.9136	0.9170	0.0034
0.36212	0.9108	0.9137	0.0029
0.43472	0.9071	0.9127	0.0056
0.46938	0.9073	0.9125	0.0052
0.49515	0.9065	0.9124	0.0059
0.65440	0.9055	0.9132	0.0077
0.66660	0.9061	0.9133	0.0072
0.78688	0.9078	0.9151	0.0073
0.80043	0.9084	0.9153	0.0069
0.86536	0.9084	0.9166	0.0082
0.93302	0.9112	0.9182	0.0070
1.0085	0.9117	0.9201	0.0084
1.0962	0.9138	0.9227	0.0089
1.1497	0.9149	0.9244	0.0095
1.2886	0.9183	0.9292	0.0109
1.5443	0.9278	0.9394	0.0116
1.8253	0.9403	0.9524	0.0121
2.1981	0.9574	0.9719	0.0145
4.3345	1.085	1.098	0.0130

$$\bar{L}_2 = -\nu RT^2 \left(\frac{\partial \Delta \ln \gamma_{\pm}}{\partial T} \right) = b(T) \sqrt{m} \qquad (59)$$

or

$$\Delta \ln \gamma_{\pm} = b'(T) \sqrt{m} \qquad (60)$$

where $b \neq b'$ and remembering that

$$\Delta\phi = \frac{1}{m} \int_0^m m \, d\Delta \ln \gamma_{\pm} \quad . \qquad (61)$$

then

$$\Delta\phi = \frac{1}{m} \, b''(T) \, m^{3/2}, \qquad (62)$$

or

$$\Delta\phi = b''(T) m^{1/2} \quad . \qquad (63)$$

The data in Table XII were therefore least-squared to an equation of the form

$$\Delta\phi = a \sqrt{m} \qquad (64)$$

The results are given in Table XIII. Also given in Table XIII are fits to two other empirical equations based on the $\sqrt{m}$ dependence but including higher terms. For this particular data set, the F- ratio test[64] requires that

$$\frac{\text{variance (1 parameter fit)}}{\text{variance (2 parameter fit)}} > 2.01 \qquad (65)$$

for either of the two parameter fits to be statistically more significant than the one parameter fit on the 95% confidence level. It follows that the fit to $\Delta\phi = a \sqrt{m} + bm$ may be discarded directly as statistically inferior. The fit to $\Delta\phi = a \sqrt{m} + b$ gives a ratio of variances equal to 2.3 when compared with the single parameter fit and at first glance is therefore marginally better. However, it is to be recalled that the statistical uncertainty of the fit to $\Delta\phi$ should have the statistical uncertainty of the ϕ_H data superposed on it

TABLE XIII

FITS OF $\Delta\phi$ TO EMPIRICAL FUNCTIONS

$\Delta\phi$ =	a	b	Variance of Fit
$a\sqrt{m}$	$8.5620 \times 10^{-3} \pm 2.629 \times 10^{-4}$		1.21×10^{-6}
$a\sqrt{m} + b$	$1.0779 \times 10^{-2} \pm 4.30 \times 10^{-4}$	$-2.0702 \times 10^{-3} \pm 3.684 \times 10^{-4}$	5.21×10^{-7}
$a\sqrt{m} + bm$	$5.2744 \times 10^{-3} \pm 7.040 \times 10^{-4}$	$3.1607 \times 10^{-3} \pm 6.525 \times 10^{-4}$	6.14×10^{-7}

since these smoothed data were employed in calculating $\Delta\phi$ from ϕ_D. This uncertainty (expressed as σ_H) varies as a function of concentration and is displayed in Figure 8 together with the $\Delta\phi$ data points and the two fits $\Delta\phi_I = a\sqrt{m}$ and $\Delta\phi_{II} = a\sqrt{m} + b$. Taking account of the ϕ_H uncertainties, it can be seen that the $\Delta\phi_{II}$ prediction of a finite intercept is not statistically valid. We therefore discard the fit $\Delta\phi_{II}$ from further consideration since theory requires that ϕ_H and ϕ_D approach unity as the concentration approaches zero (thus $\Delta\phi$ approaches 0 at $m = 0$). The argument can be expressed more simply, albeit more approximately. With the variance for $\Delta\phi_{II} = 5.2 \times 10^{-7}$, the uncertainty of a single point is $\sim 7 \times 10^{-4}$ and similarly for ϕ_H the variance = 1.3×10^{-6} and $\sigma_H \cong 1 \times 10^{-3}$. The total is $(5 \times 10^{-7} + 1.3 \times 10^{-6})^{1/2} \cong 1.4 \times 10^{-3}$ and on the 95% confidence level of 2σ is $\sim 3 \times 10^{-3}$ which is larger than the intercept obtained in $\Delta\phi_{II}$.

In terms of the extended Debye-Hückel theory, separate equations for ϕ_H and ϕ_D can be written (Equation 12, p 35). Subtracting these equations gives the result,

$$\Delta\phi = \phi_H - \phi_D = DH_H - DH_D + (1/2\Delta B)I + (2/3\Delta C)I^2 + (3/4\Delta D)I^3 + \text{---}. \quad (66)$$

The results of the fits to different forms of the Debye-Hückel equation are given in Table XIV. The value of a°_H was fixed at 4.45 A° from the fit of ϕ_H's (p 62) derived from freezing point depressions. The fit using only the leading terms ($DH_H - DH_D$) is not good, and the value of a°_D shows an unreasonably large isotope effect (p 44). The addition of the first empirical term improves the fit significantly, but again the value of Δa° is not reasonable. Addition of the second empirical term does not improve the fit but the value of a°_D changes again. The

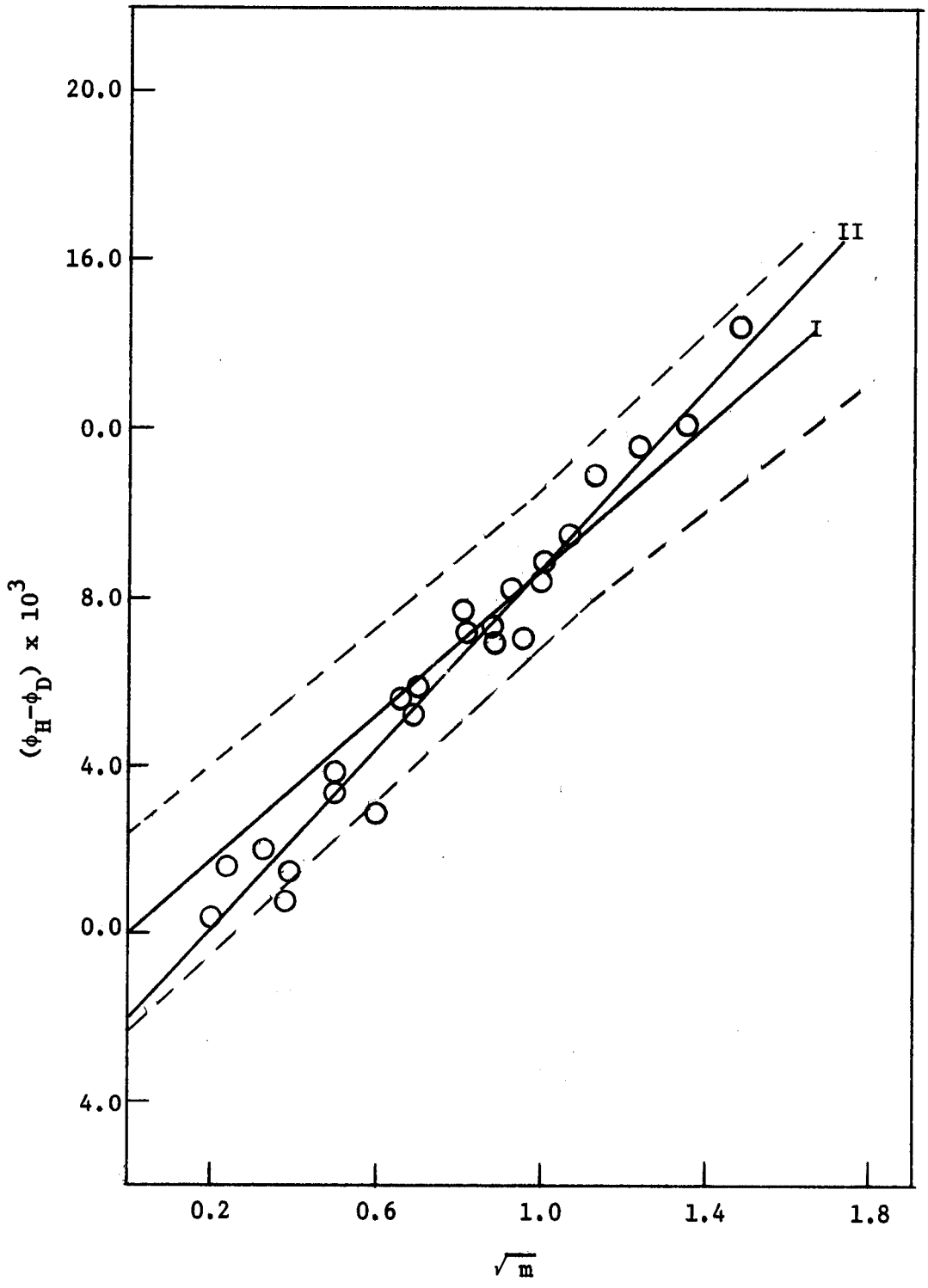

Figure 8. Fit of $\phi_H-\phi_D(\Delta\phi)$ at 3.82°.

I is fit to $\Delta\phi = a\sqrt{m}$; II is fit to $\Delta\phi = a\sqrt{m} + b$; dashed line is error band (2σ) for fit I.

TABLE XIV

FITS OF $\Delta\phi$ TO FORMS OF THE EXTENDED DEBYE-HÜCKEL EQUATION

$\Delta\phi$	a_D°	1/2 ΔBm	2/3 ΔCm	Variance of Fit
$DH_H - DH_D$	$4.0676 \times 10^{-8} \pm 1.94 \times 10^{-10}$			3.36×10^{-6}
$DH_H - DH_D$ + 1/2 ΔBm	$4.2875 \times 10^{-8} \pm 2.28 \times 10^{-10}$	$4.7703 \times 10^{-3} \pm 4.431 \times 10^{-4}$		5.74×10^{-7}
$DH_H - DH_D$ + 1/2 ΔBm + 2/3 ΔCm^2	$4.3512 \times 10^{-8} \pm 4.989 \times 10^{-10}$	$7.2645 \times 10^{-3} \pm 1.780 \times 10^{-3}$	$-9.3406 \times 10^{-4} \pm 6.488 \times 10^{-4}$	5.48×10^{-7}
1/2 ΔBm + 2/3 ΔCm^2		$1.1205 \times 10^{-2} \pm 5.06 \times 10^{-4}$	$-2.2879 \times 10^{-3} \pm 3.249 \times 10^{-4}$	6.71×10^{-7}

parameters from all these fits are highly correlated ($\sim$ 0.9) which makes it difficult if not impossible to give a physical interpretation to a°_{D}. The fit using the first two empirical terms and setting $DH_H - DH_D = 0$ describes the data as well as any of the previous ones. Although some forms of the Debye-Hückel theory fit the data well, it is to be emphasized that none of the fits (including those with two or more parameters) are statistically better than the empirical one parameter fit of $\Delta\phi$ to a $\sqrt{m}$.

8. Calculation of $\Delta\phi$ at Other Temperatures

The isotope effect on ϕ at temperature other than 276.97°K (3.82°) can be calculated using the isotope effect on $\bar{L}_1$, $\Delta\bar{L}_1$. Equation 22 (p 42) gives $\Delta\bar{L}_1$ as a function of temperature and concentration. Equations analogous to Equation 48 (p 58) and Equation 49 (p 59) can be written for the isotope effect.

$$\left(\frac{\partial \Delta \ln a}{\partial T}\right) = - \frac{\Delta\bar{L}_1}{RT^2} \tag{67}$$

$$\Delta\phi = - \frac{\Delta \ln a_1 \ (55.508)}{\nu m} \tag{68}$$

Substitution of Equation 22 for $\Delta\bar{L}_1$ followed by integration of Equation 67 from 276.97°K to the temperature of interest, T, gives an equation for the isotope effect on the natural logarithm of a_1, $\Delta \ln a_1$, at T. Solving Equation 68 for $\Delta \ln a_1$ and substituting gives

$$\Delta\phi_T = \Delta\phi_{276.97} + \frac{\sqrt{m}}{3R\nu}\left[d\left(\frac{1}{T} - \frac{1}{276.97}\right) - e \ln \frac{T}{276.97}\right] . \tag{69}$$

Here, d and e are the parameters from Equation 21 (p 42). Values of $\Delta\phi$ at rounded temperatures and concentrations are presented in

Appendix II. The temperature dependence is shown graphically in Figure 9.

9. Comparisons with Literature

Values of $\Delta\phi$ calculated from the vapor pressure isotope effects on NaCl solutions have been reported by Van Hook and coworkers.[9] Measurements of the vapor pressure isotope effect were made at 1.1, 2.9, 4.0 and 5.5 molal and from 0 to 90°. The data were interpreted in terms of the extended Debye-Hückel theory. By making the assumption that there is no isotope effect on the a° parameter, the authors showed that the contribution of the DH terms is small ($\sim 10^{-6}$) compared with their experimental error. Within experimental error their data for NaCl was fit using only the first empirical term of the extended theory.

$$\Delta\phi = bm \qquad (70)$$

Here b is equivalent to the quantity $1/2\Delta B$ used in Equation 66 (p 74). Figure 10 shows a comparison of $\Delta\phi$ from the vapor pressure measurements with $\Delta\phi$ from the present work. In the interest of clarity, the original vapor pressure data points rather than the smoothed values were employed. The vapor pressure points shown in Figure 10 were calculated at 40° from the original data ranging from 30 to 50°. They were corrected to 40° using $\Delta\bar{L}_1$ values of Equation 22 (p 42). The comparison is made at 40° because the vapor pressure becomes more reliable at higher temperatures. The agreement is satisfactory considering that the vapor pressure measurements were made at high NaCl concentrations and extend over only a half decade in the concentrations, while the freezing point measurements range to low concentration and extend over two decades.

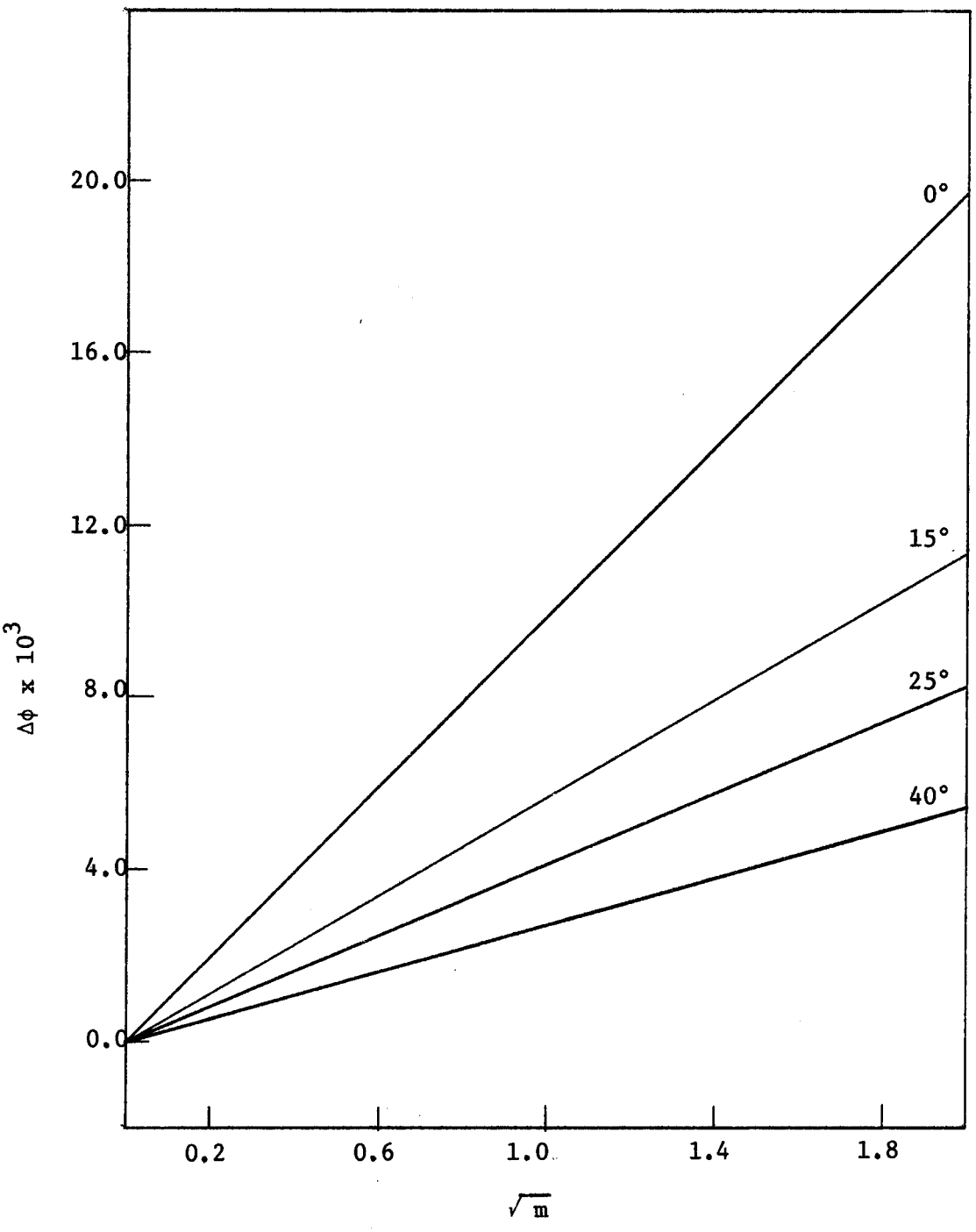

Figure 9. Temperature dependence of $\Delta\phi$.

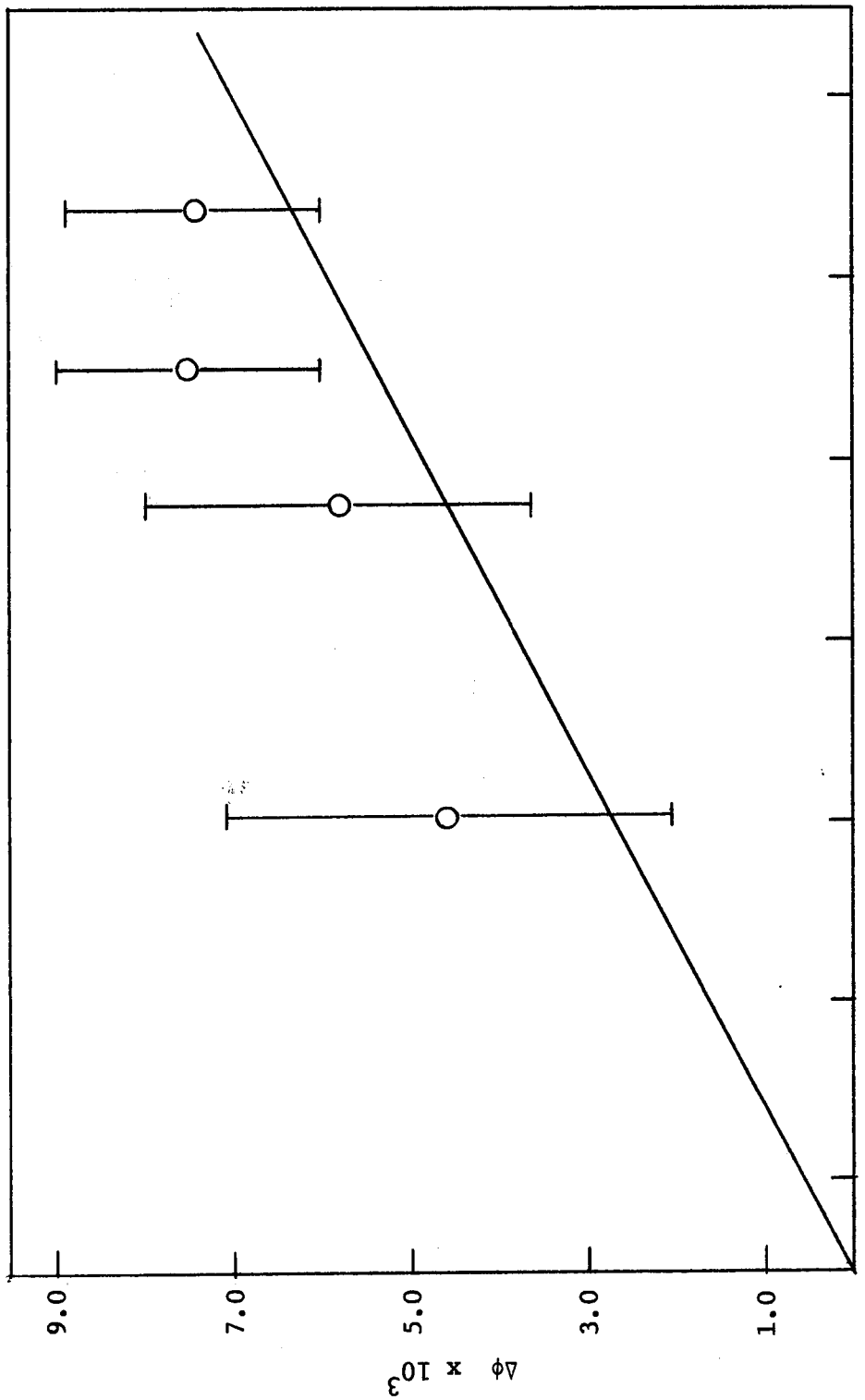

Figure 10. Comparison (at 40°) of $\Delta\phi$ from vapor pressure[9] (circles) with $\Delta\phi$ from present work (line).

The experimental precision of the vapor pressure measurements is low relative to the magnitude of the isotope effects. The technique is being pushed to its limit. The freezing point measurements are of greater precision and indicate a different concentration dependence than that assumed in the work up of the vapor pressure data. The incorrect assumption of the $\Delta\phi = bm$ concentration dependence coupled with an empirical form for the temperature dependence of b makes the smoothed vapor pressure data suspect for our purposes, and it was for this reason that the comparison is made with the original data points insofar as possible.

Schrier and Schrier[11] determined $\Delta \ln \gamma_{\pm}$ at 25° for NaCl solutions by using a glass electrode. Their measurements were designed to determine an average slope, $d\Delta \ln \gamma_{\pm}/dm$, by measuring the change in potential for a net change in the NaCl concentration (usually a factor of two). As with the vapor pressure, the e.m.f. measurements are most reliable at high concentration although low concentration (0.11 molal) slopes are reported. The authors concluded that within experimental error $d\Delta \ln \gamma_{\pm}/dm$ was not a function of concentration. Thus,

$$\Delta \ln \gamma_{\pm} = 2bm \qquad (71)$$

and

$$\Delta\phi = bm \quad . \qquad (72)$$

The derived value of b was found to be consistent with that from the vapor pressure work (p 78). No direct comparison (point by point) can be made with the present work, but it appears that the concentration dependence predicted by Schrier below 1 m does not agree with that of the present work (although agreement improves as the concentration increases). This is perhaps a consequence of their incorrect assumption that $\Delta\phi = bm$.

Kerwin[12] determined $\Delta\phi$ using isopiestic methods. His results do not agree with the present work or with other workers. A plausible explanation is that his isopiestic reference, $ZnSO_4$,[65] is in error.

10. Calculation of ΔG_2°

The isotope effect on the standard free energy of transfer of NaCl, ΔG_2°, from D_2O to H_2O can be calculated from the present data with the aid of the isotope effect on the solubility of NaCl measured by Eddy and Menzies.[66]

$$G_{2H}^\circ - G_{2D}^\circ = \Delta G_2^\circ = -2RT\ln\left(\frac{m_H\gamma_H(H)}{m_D\gamma_D(D)}\right)$$

$$= -2RT\left[\ln\left(\frac{m_H}{m_D}\right) + \ln\left(\frac{\gamma_H(H)}{\gamma_H(D)}\right) + \ln\left(\frac{\gamma_H(D)}{\gamma_D(D)}\right)\right] . \quad (73)$$

Here, m_H and m_D are the solubility of NaCl in H_2O and D_2O. $\gamma_H(D)$ refers to the activity coefficient in H_2O at concentration m_D. The term $\ln(\gamma_H(H)/\gamma_H(D))$ was calculated using the activity coefficients of Gibbard, Scatchard, Rosseau, and Creek.[56] The last term was calculated from $\Delta\phi$ as follows:

$$\Delta\phi = \frac{1}{m}\int_0^m d\Delta\ln\gamma_\pm , \quad (74)$$

but from this work $\Delta\phi = a\sqrt{m}$. After differentiation, integration, and rearrangement

$$\Delta\ln\gamma_\pm = \ln\left(\frac{\gamma_H}{\gamma_D}\right) = 3a\sqrt{m} \quad (75)$$

The value of a at different temperatures can be determined from the data for $\Delta\phi$ given in Appendix II. The values of ΔG_2° at 25° (-173 cal $mole^{-1}$) and 50° (-131 cal $mole^{-1}$) agree within 1 cal $mole^{-1}$ with those

calculated from the vapor pressure measurement. However, most of the effect is determined by the isotope effect on the solubility.

CHAPTER IV

DISCUSSION

A. Introduction

The more interesting and significant results established in this work may be ranked in decreasing order of importance as follows:

1. The observation that the limiting concentration dependence of both the enthalpy ($\bar{L}_2$) and the osmotic coefficient (ϕ) isotope effects is proportional to $\sqrt{m}$.
2. The analysis of the reliability of the isotope effect data for the NaCl system (both activity and heat data) established it firmly as the most suitable reference (isopiestic) system over a broad temperature range.
3. A new and reliable value for the heat of fusion of D_2O is reported.
4. The analysis of presently available activity data at low concentration resulted in a more realistic judgment of the reliability of these data for the NaCl-H_2O system.

In the material which follows these topics will each be briefly discussed except that items 2 and 4 will be treated together because they are so intimately related. The order of treatment is 3, 4, 2, 1.

B. Heat of Fusion of D_2O

The heat of fusion of D_2O (-1507 ± 3 cal mole^{-1}) determined by the intercept of the isotope effect on the freezing point depression

is as good or better than that determined calorimetrically. This new value will be of use in the interpretation of the vapor pressure isotope effect of the pure isotopic waters. This has been discussed in detail by Jancso and Van Hook.[9] Briefly, accurate information on the isotope effect on the change in slope of vapor pressure curves on phase change (the enthalpies of fusion) will allow more realistic assignment of the important lattice modes, particularly librational modes in the two phases assuming the interpretation proceeds within the framework of the average cell model. Alternatively, this more precise datum may allow for refinements in the model used to describe vapor pressure isotope effects of the substituted waters.

C. Reliability of the Data

1. H_2O Data

a. Heat data. The values of $\bar{L}_{2H}$ determined from differential heats of solution (at 5, 15, 25, and 40°) are in good agreement with literature data. The data (present work plus selected literature values) are fit well to a form of the extended Debye-Hückel equation (p 33). In a second fit of the $\bar{L}_{2H}$ data, the value of $(\partial \ln a^\circ_H/\partial T)$ was determined for NaCl in H_2O and is a factor of $\sim$ 40 smaller than the corresponding value determined for HI by Gier and Vanderzee. No physical interpretation can be given to $(\partial \ln a^\circ_H/\partial T)$.

A Gibbs-Duhem integration gives values of $\bar{L}_{1H}$ which are in good agreement with available literature data. Also, when extrapolated to 0°, the values of $\bar{L}_{1H}$ agree well with those measured by Young and Machin.[41]

b. Freezing point data. The measurement of the freezing point depression is considered to be the best method for determining the solvent activity or osmotic coefficient at low salt concentration. However, a careful error analysis of all the available H_2O data shows that at the freezing point of the solution the osmotic coefficient is not known to better than $\pm$ 0.001 unit at any concentration.

The calculation of the osmotic coefficient at temperatures other than the freezing point of the solution introduces additional error because $\bar{L}_{1H}$ is not known to necessary accuracy. In fact, there are no direct measurements of $\bar{L}_{1H}$ below 0°. Thus, the correction of the osmotic coefficient to 0° involves an extrapolation of the $\bar{L}_{1H}$ data to the freezing point of the solution. As the concentration of salt increases the freezing point of the solution decreases and the extrapolation used to determine $\bar{L}_{1H}$ becomes longer and less precise and leads to significant errors in the osmotic coefficient at 0° for concentrations greater than 1 m (see Figure 7, p 63). The further correction of the osmotic coefficient to 25° does not result in a substantial increase in the error because values of $\bar{L}_{1H}$ have been measured for this temperature range. Measured values of $\bar{L}_{1H}$ below 0° are needed for the calculation of high precision ($\sim \pm$ 0.001) osmotic coefficients for concentrations greater than 1 m at temperatures other than the freezing point of the solution. Until such measurements are complete it is inaccurate to claim (as many authors have) that activities derived from freezing point measurements are thermodynamically consistent with those obtained from vapor pressure data, at least above 1 m.

2. Isotope Effects

a. Heat data. The isotope effect on $\bar{L}_2$ derived from differential heats of solution measurements are consistent with the isotope effect on the heats of dilution available in the literature (all at 25°) and those of the present work (see Table VI, p 49). All the dilution data are for high concentration ($m \geq 1$) while the differential data extend from 0.01 to 4 m. Although not as pertinent as values of $\Delta\bar{L}_2$, the isotope effect on the integral heat of solution of the present work (see Table VII, p 52) are in excellent agreement with literature values at 25°.

The calculation (using data of present work) of the isotope effect on the partial molal heat capacity at infinite dilution and 25° agrees well with the directly measured value of Desnoyers and coworkers.[46] Also, values of $\Delta\bar{J}_2$ calculated from the present work and from the data of Desnoyers agree well at 1 m and 25°. The agreement with directly measured heat capacities lends credence to the heat data because the calculation of heat capacities from measured enthalpies is a stringent test of the data.

Whereas previous heat data on the isotope effect have been limited to 25°, the data presented here cover a wide temperature range and are of theoretical importance because the structure of solutions changes significantly with temperature. Desnoyers[46] and Friedman[3] have developed a qualitative "cosphere" model for aqueous solution, and the heat data of the present work are in general agreement with that model. It is to be anticipated however that the broad range of temperature and concentration scaled by the present data will be of material

aid in refining or modifying that particular model or similar models.

b. Osmotic coefficients. The errors encountered in calculating the osmotic coefficient for H_2O, ϕ_H, at temperatures other than the freezing point of the solution have been discussed previously (see p 64). It was noted that the correction of ϕ_H to 0° does not involve significant errors (error < 0.001) for concentrations less than 1 m. The additional small correction to 3.82° does not result in a significant increase in the error. Thus, for m > 1 both $\phi_H^{3.82}$ and $\phi_D^{3.82}$ contain errors which result from the fact that $\bar{L}_{1H}$ and $\bar{L}_{1D}$ are not known below the respective freezing points of the pure solvents. Since the isotope effect on the freezing point depression is small relative to the actual freezing point depression, the lengths of the extrapolation to determine $\bar{L}_{1H}$ and $\bar{L}_{1D}$ are equal for all practical purposes. It follows that the errors in $\bar{L}_{1H}$ and $\bar{L}_{1D}$ should be approximately equal and of the same sign. Thus, the errors in ϕ_H and ϕ_D tend to cancel in the calculation of $\Delta\phi = \phi_H - \phi_D$. At 2m (the highest concentration for which freezing point depressions in H_2O and D_2O were measured) the total error in $\phi_H^{3.82}$ is at most $\pm$ 0.003, and the corresponding error in $\Delta\phi$ (at 2 m) is estimated as less than $\pm$ 0.001.

Values of $\Delta\phi$ derived from the freezing point depressions agree with the previous vapor pressure and e.m.f. measurements at high concentration (m > 1). Since the isotope effects, $\Delta\phi$, are small, the vapor pressure and e.m.f. methods are only capable of yielding reliable results for concentration greater than 1 m.

The isotope effect on the partial molal enthalpy of the solvent, $\Delta\bar{L}_1$, permits calculation of $\Delta\phi$ from 0 to 40°. These values of $\Delta\phi$ can be combined with values of ϕ_H from other methods (freezing point measurements give reliable values of ϕ_H for $m \lesssim 1$) to give values of ϕ_D. Our values of ϕ_D calculated in this fashion are the best available. They establish the NaCl-D_2O system as an isopiestic standard for heavy water solutions. While other salts could be investigated using the methods employed in the present work, the amount of work is prohibitive, and the use of isopiestic measurements will have a definite advantage in future investigations.

c. The $\sqrt{m}$ concentration dependence. The isotope effects on $\bar{L}_2$ and ϕ found in the present work are proportional to $\sqrt{m}$ within experimental error. Concentration dependencies (i.e., m or $m + m^2$) assumed by earlier authors to describe measurements at high concentrations ($m > 1$) result in significant calculated differences for thermodynamic properties from the present formulation. This is because the calculations are sensitive to the specific form used in extrapolating to infinite dilution. An example was given (p 54) for the calculation of ΔL_2^s.

In their present form the Debye-Hückel equations for $\Delta\bar{L}_2$ and $\Delta\phi$ do not describe the data in a realistic manner. If the physical interpretation that a° is the distance of closest approach is invoked, then the isotope effect on a° determined from least-square fits to the data are not physically reasonable (see p 44). Also the incorporation of one or more of the empirical terms is needed to describe the data. The resulting fits (requiring at least 2 parameters) are not statistically

better than fits to the much simpler empirical equations. It is obvious that in its present form the Debye-Hückel equation can not be used to interpret the isotope effect data.

Although various modifications of the cosphere model[67] have been used to rationalize solvent isotope effects,[3,46] the interpretations have been highly qualitative. It is difficult to rationalize the observed $\sqrt{m}$ dependence with this approach. In a modification of this general approach, however, Van Hook[68] has considered possible isotope effects on the coordination number of the ions (i.e., on cosphere size). This assumption is important as previous authors using the cosphere model have ignored this complication. In early efforts Van Hook has parametrically incorporated the isotope effect on the coordination number into the leading terms of the Debye-Hückel equation by considering a concentration dependent dielectric constant. That is he assumes, following Pottel,[69] that $\varepsilon_s = \varepsilon_o$ (f(s)) where ε_s and ε_o are the dielectric constants of the solution and pure solvent, respectively, and f(s) is a concentration dependent weighting function which can be obtained from nmr measurements. f(s) is a simple function of the fraction of solvent molecules which are ion-bound, i.e., the cosphere size or coordination number. Van Hook's preliminary calculation involves parameterization around $\Delta f(s)$, the isotope effect on f(s), and shows important contributions from leading terms proportional to $\sqrt{m}$. This is encouraging in light of the present experimental observations. Obviously much theoretical work remains, but it is beyond the scope of the present, primarily experimental, contribution.

CHAPTER V

CONCLUSIONS

1. The heat of fusion of D_2O as calculated from the isotope effect on the freezing point depression is -1507 $\pm$ 3 cal mole^{-1} at 3.82°.
2. Isotope effects on ϕ and $\bar{L}_2$ are proportional to $\sqrt{m}$.
3. Values of $\Delta\phi$, $\Delta\bar{L}_1$, and $\Delta\bar{L}_2$ are reported from 0-5 m and 0-40°. These values for the isotope effects are the best available and establish this system as a suitable isopiestic reference for solutions with heavy water as solvent.

LIST OF REFERENCES

LIST OF REFERENCES

1. F. Franks, Ed., "Water a Comprehensive Treatise," Vol. I, II, III, Plenum Press, New York, N. Y., 1973.

2. E. M. Arnett and D. R. McKelvey in "Solute Solvent Interactions," J. F. Coetzu and C. D. Ritchie, Eds., Interscience Publishers, New York, N. Y., 1969, pp. 343-398.

3. H. L. Friedman and C. V. Krishnan in "The Physics and Physical Chemistry of Water," Vol III, F. Franks, Ed., Plenum Press, New York, N. Y., 1973, pp. 1-118.

4. J. Bigeleisen, M. W. Lee, and F. Mandel, Ann. Rev. Phys. Chem., 24, 407 (1973).

5. G. Jancso and W. A. Van Hook, Chem. Reviews, 74, 689 (1974).

6. M. Wolfsberg, J. Chem. Phys., 59, 2043 (1973).

7. A. Y. Fang and W. A. Van Hook, J. Chem. Phys., 60, 3513 (1974).

8. J. Bigeleisen, J. Chim. Phys., 61, 87 (1964).

9. J. Rupezin, G. Jakli, G. Jancso, and W. A. Van Hook, J. Phys. Chem., 76, 743 (1972).

10. G. Jakli, T. C. Chan, and W. A. Van Hook, J. Soln. Chem., 4, 71 (1975).

11. M. Y. Schrier and E. E. Schrier, J. Chem. Thermodynamics, 5, 811 (1973).

12. R. E. Kerwin, Ph.D. Dissertation, University of Pittsburgh, 1964.

13. C. Robertson and V. K. LaMer, J. Phys. Chem., 35, 1953 (1939).

14. G. Scatchard, P. T. Jones, and S. S. Prentiss, J. Amer. Chem. Soc. 54, 2676 (1932).

15. T. W. Richards, J. Amer. Chem. Soc., 25, 291 (1903).

16. Victory Engineering Company, "Thermistor Data Book," 1953, p. 19.

17. Donald Robertson and Kasper A. Walch in "Temperature Its Measurement and Control in Science and Industry," Vol. II, Charles M. Herzfeld and F. G. Brickwedde, Eds., Reinhold Publishing Corporation, New York, N. Y., 1962, pp. 291-299.

18. T. W. Richards, as quoted by J. R. Partington, "Textbook of Inorganic Chemistry," McMillian, London, 1950, p. 91.

19. C. W. Foulk, H. V. Moyer, and W. M. MacNevin, "Quanitative Chemical Analysis," 1st Ed., McGraw-Hill Book Co., New York, N. Y., 1952, p. 97.

20. J. S. Beekley and H. S. Taylor, J. Amer. Chem. Soc., 29, 942 (1925).

21. G. Scatchard and S. S. Prentiss, J. Amer. Chem. Soc., 55, 4355 (1933).

22. M. H. Lietzke, ORNL Report No. 3259, Oak Ridge National Laboratory, Oak Ridge, Tennessee, April 1962.

23. P. Debye and E. Hückel, Physic. Z., 24, 185, 334 (1923).

24. P. Debye and E. Hückel, Physic. Z., 25, 97 (1924).

25. H. S. Harned and B. B. Owen, "The Physical Chemistry of Electrolyte Solution," 2nd Ed., Reinhold Publishing Corporation, New York, N. Y., 1954, p. 379.

26. E. Hückel, Physik. Z., 93 (1925).

27. R. W. Stoughton and M. H. Lietzke, J. Chem. Eng. Data, 10, 254 (1965).

28. N. Bjerrum, Z. Elektrochem., 24, 259 (1907).

29. M. H. Lietzke and R. W. Stoughton, J. Phys. Chem., 65, 508 (1961).

30. R. W. Stoughton and M. H. Lietzke, J. Chem. Eng. Data, 12, 101 (1967).

31. F. J. Millero, J. Phys. Chem., 74, 356 (1970).

32. Y. S. Choi and O. D. Bonner, Z. Physic. Chem., 87, 188 (1973).

33. G. S. Kell, J. Chem. Eng. Data, 12, 66 (1967).

34. G. A. Vidulich, D. F. Evans, and R. L. Kay, J. Phys. Chem., 71, 656 (1967).

35. C. M. Criss and J. W. Cobble, J. Amer. Chem. Soc., 83, 3223 (1961).

36. E. A. Gulbransen and A. L. Robinson, J. Amer. Chem. Soc., 56, 2637 (1934).

37. V. B. Parker, Thermal Properties of Aqueous Uni-Univalent Electrolytes, NSRDS-NBS2 (1965).

38. D. D. Ensor and H. L. Anderson, J. Chem. Eng. Data, 18, 205 (1973).

39. C. E. Vanderzee and L. J. Gier, J. Chem. Thermodynamics, 6, 441 (1974).

40. J. R. Britton, R. B. Kriegh and L. W. Rutland, "Univeristy Mathematics," W. H. Freeman and Company, San Francisco, California, 1965, p. 570.

41. T. F. Young and J. S. Machin, J. Amer. Chem. Soc., 58, 2254 (1936).

42. S. J. Cyvin, "Molecular Vibrations and Mean Square Amplitudes," American Elsevier Publishing, New York, N. Y., 1968, p. 205.

43. I. M. Klotz, "Chemical Thermodynamics," Prentiss-Hall, Inc. Englewood Cliffs, N. J., 1957, p. 218.

44. R. H. Wood, R. A. Rooney, and J. N. Braddock, J. Phys. Chem., 73, 1673 (1969).

45. Yung-Chi Wu and Harold L. Friedman, J. Phys. Chem., 70, 166 (1966).

46. J. E. Desnoyers, R. Francescon, P. Picker, and C. Jolicoeur, Can. J. Chem., 49, 3460 (1971).

47. D. H. Davies and G. C. Benson, Can. J. Chem., 43, 3100 (1965).

48. E. Lange and W. Martin, Z. Physic. Chem., A180, 233 (1937).

49. J. Fortier, P. R. Philip, and J. E. Desnoyers, J. Soln. Chem., 3, 523 (1974).

50. G. N. Lewis, M. Randall, K. S. Pitzer, and L. Brewer, "Thermodynamics," 2nd Ed., McGraw-Hill, New York, N. Y., 1961, p. 375, 382.

51. F. Momicchioli, O. Devoto, G. Cocco, and G. Grandi, Ber. Bunsenges. Phys. Chem., 74, 59 (1970).

52. H. F. Gibbard and A. F. Gossmann, J. Soln. Chem., 3, 385 (1974).

53. N. S. Osborne, J. Res. Natl. Bur. Standards, 23, 643 (1939).

54. N. S. Osborne, H. F. Stimson and D. C. Ginnings, J. Res. Natl. Bur. Standards, 23, 197 (1939).

55. H. C. Dickinson and N. S. Osborne, Bull. Natl. Bur. Standards, 12, 49 (1915).

56. H. F. Gibbard, G. Scatchard, R. A. Ronsseau, and J. L. Creek, J. Chem. Eng. Data, 19, 281 (1974).

57. R. F. Platford, J. Chem. Eng. Data, 18, 215 (1973).

58. R. A. Robinson and R. H. Stokes, "Electrolyte Solution," 2nd Ed., Academic Press Inc., New York, N. Y., 1959, p. 483.

59. T. F. Young, Chem. Rev., 13, 103 (1933).

60. E. A. Long and J. D. Kemp, J. Amer. Chem. Soc., 58, 1829 (1936).

61. F. D. Rossini, J. W. Knowlton, H. L. Johnston, J. Res. Natl. Bur. Standards, 24, 369 (1940).

62. A. H. Crockett and A. Ferguson, The London, Edinburgh and Dublin Philasophical Magazine and Journal of Science, Ser. 1, 29, 193 (1940).

63. Ya. Z. Kazavchinski, P. M. Kessel'man, V. A. Kirillin, S. L. Rivkin, A. E. Sheindlin, E. E. Shpil'rain, V. V. Sychev, and D. L. Trimrot, "Heavy Water Thermophysical Properties," Keter Press, Jerusalem, Israel, 1971, p. 78.

64. W. J. Youden, "Statistical Methods for Chemists," John Wiley and Sons, New York, N. Y., 1951, p. 20.

65. J. C. Rasiah, Thesis, University of Pittsburgh, 1965.

66. R. D. Eddy and A. W. C. Menzies, J. Phys. Chem., 44, 207 (1940).

67. H. S. Frank and M. W. Evans, J. Chem. Phys., 13, 507 (1945).

68. W. A. Van Hook, University of Tennessee, Knoxville, Tennessee, personal communication.

69. R. Pottel in "The Physics and Physical Chemistry of Water," Vol. III, F. Franks, Ed., Plenum Press, New York, N. Y., 1973, pp. 401-431.

APPENDICES

APPENDIX I

CALIBRATION DATA FOR THERMISTOR AND PLATINUM THERMOMETER

The platinum thermometer (T-1) was calibrated using standard methods.[17] The thermometer resistance and calibration temperatures (1948 International Temperature Scale) are:

$R = 25.5530\ \Omega$, $T = 273.150°K$,

$R = 35.6077\ \Omega$, $T = 373.377°K$, and

$R = 30.6132\ \Omega$, $T = 323.190°K$.

The resulting constants for the Callendar Equation are: $R_o = 25.5530\ \Omega$, FI = 10.0322, and $\delta = 1.595$.

This platinum thermometer was used to calibrate the thermistor. The temperature (T) and resistance readings (R) are given in Table XV. The data of Table XV were least-squared to

$$R = A \exp\ (B/T + C/T^2)$$

and the resulting parameters are: $A = 3.52507 \times 10^{-3} \pm 8.708 \times 10^{-5}$, $B = 4.48159 \times 10^{3} \pm 1.36 \times 10^{1}$, and $C = -1.45023 \times 10^{5} \pm 1.9 \times 10^{3}$. The variance of fit was 1.23×10^{-1}. The thermistor was one leg of a Wheatstone bridge in which the other three resistances were fixed at 6735 ohms.

TABLE XV

CALIBRATION OF THERMISTOR

T(°K)	R(ohms)
268.284	8450.3
268.786	8252.5
269.291	8058.8
269.830	7857.4
270.935	7463.3
271.465	7281.7
272.515	6936.9
273.185	6726.4
273.953	6494.7
274.567	6315.8
274.928	6212.7
275.472	6063.0
275.832	5965.2
276.063	5902.5
276.501	5787.7
277.316	5580.1
277.896	5437.8
278.685	5250.3
279.462	5073.3
280.128	4926.9
281.696	4600.6
282.298	4481.9
283.305	4290.5
284.271	4116.6
285.057	3980.4
286.035	3818.2
287.063	3656.0

TABLE XV (Continued)

T(°K)	R(ohms)
288.114	3498.3
289.163	3348.4
290.407	3180.0

APPENDIX II

TABULAR SUMMARY OF ISOTOPE EFFECTS

TABLE XVI

SUMMARY OF ISOTOPE EFFECTS[a] IN H_2O-D_2O-NaCl SYSTEM

t, °C	m	$\bar{L}_{2H}$	$\Delta\bar{L}_2$	$\bar{L}_{1H}$	$\Delta\bar{L}_1$	ϕ_H[b]	$\Delta\phi \times 10^3$
0	0.1	-11.4	100.0	0.051	-0.060	0.931_9	$3._1$
	0.2	-92.8	142.0	0.274	-0.171	0.920_2	$4._4$
	0.3	-179.0	174.0	0.665	-0.314	0.914_6	$5._4$
	0.4	-266.0	201.0	1.21	-0.487	0.911_7	$6._2$
	0.5	-351.0	225.0	1.91	-0.676	0.910_3	$7._0$
	0.6	-435.0	247.0	2.74	-0.889	0.910_0	$7._6$
	0.7	-517.0	267.0	3.70	-1.12	0.910_6	$8._2$
	0.8	-596.0	285.0	4.77	-1.37	0.911_8	$8._8$
	0.9	-672.0	302.0	5.95	-1.63	0.913_0	$9._3$
	1.0	-747.0	319.0	7.22	-1.91	0.915_7	$9._8$
	1.2	-888.0	349.0	10.0	-2.51	0.921_2	$10._0$
	1.4	-1020.0	377.0	13.1	-3.17	0.928_1	$11._7$
	1.6	-1142.0	403.0	16.4	-3.87	0.936_2	$12._5$
	1.8	-1255.0	427.0	19.9	-4.62	0.945_2	$13._2$
	2.0	-1358.0	450.0	23.4	-5.41	0.955_1	$13._9$
	2.6	-1611.0	514.0	33.8	-8.02	0.988_5	$15._9$
	3.0	-1732.0	552.0	39.8	-9.94	1.012_8	$17._1$
	3.6	-1832.0	604.0	45.6	-13.1	1.050_0	$18._7$
	4.0	-1840.0	640.0	46.0	-15.3	1.074_1	$19._7$
	4.6	-1749.0	683.0	38.7	-18.9	1.107_1	$21._1$

TABLE XVI (Continued)

t, °C	m	$\bar{L}_{2H}$	$\Delta\bar{L}_2$	$\bar{L}_{1H}$	$\Delta\bar{L}_1$	ϕ_H [b]	$\Delta\phi \times 10^3$
15	0.1	54.5	62.9	0.042	-0.038	0.932_7	$1._8$
	0.2	16.5	89.0	0.111	-0.107	0.922_8	$2._5$
	0.3	-30.6	109.0	0.325	-0.196	0.919_0	$3._1$
	0.4	-80.3	126.0	0.641	-0.303	0.917_8	$3._6$
	0.5	-131.0	141.0	1.05	-0.423	0.918_2	$4._0$
	0.6	-181.0	154.0	1.55	-0.555	0.919_5	$4._4$
	0.7	-231.0	167.0	2.14	-0.700	0.921_6	$4._8$
	0.8	-280.0	178.0	2.80	-0.854	0.924_3	$5._1$
	0.9	-327.0	189.0	3.53	-1.02	0.927_4	$5._4$
	1.0	-373.0	199.0	4.33	-1.19	0.930_9	$5._7$
	1.2	-462.0	218.0	6.09	-1.57	0.939_0	$6._2$
	1.4	-546.0	235.0	8.05	-1.98	0.948_1	$6._7$
	1.6	-624.0	252.0	10.2	-2.42	0.958_2	$7._2$
	1.8	-696.0	267.0	12.4	-2.88	0.969_0	$7._6$
	2.0	-762.0	281.0	14.7	-3.38	0.980_4	$8._1$
	2.6	-929.0	321.0	21.6	-5.01	1.016_8	$9._2$
	3.0	-1012.0	345.0	25.8	-6.20	1.041_9	$9._9$
	3.6	-1091.0	378.0	30.5	-8.16	1.078_2	$10._8$
	4.0	-1111.0	398.0	32.0	-9.56	1.100_2	$11._4$
	4.6	-1090.0	427.0	30.3	-11.8	1.127_5	$12._2$
	5.0	-1036.0	445.0	25.7	-13.4	1.140_3	$12._7$
25	0.1	93.9	37.7	-0.022	-0.023	0.932_5	$1._3$
	0.2	78.4	53.3	0.025	-0.064	0.923_3	$1._8$
	0.3	51.5	65.3	0.149	-0.118	0.920_2	$2._3$
	0.4	20.4	75.4	0.348	-0.181	0.919_8	$2._6$
	0.5	-12.5	84.3	0.618	-0.253	0.920_9	$2._9$
	0.6	-45.9	92.4	0.953	-0.333	0.922_9	$3._2$
	0.7	-79.5	99.8	1.35	-0.419	0.925_6	$3._5$
	0.8	-113.0	107.0	1.80	-0.513	0.928_9	$3._7$
	0.9	-145.0	113.0	2.30	-0.611	0.932_6	$3._9$

TABLE XVI (Continued)

t, °C	m	$\bar{L}_{2H}$	$\Delta\bar{L}_2$	$\bar{L}_{1H}$	$\Delta\bar{L}_1$	ϕ_H[b]	$\Delta\phi \times 10^3$
25	1.0	-177.0	119.0	2.85	-0.717	0.936_7	$4._1$
	1.2	-239.0	131.0	4.08	-0.941	0.945_8	$4._5$
	1.4	-296.0	141.0	5.44	-1.19	0.955_9	$4._9$
	1.6	-350.0	151.0	6.90	-1.45	0.966_8	$5._2$
	1.8	-400.0	160.0	8.43	-1.73	0.978_3	$5._5$
	2.0	-446.0	167.0	10.0	-2.02	0.990_3	$5._9$
	2.6	-560.0	192.0	14.7	-3.01	1.028_1	$6._7$
	3.0	-616.0	207.0	17.6	-3.72	1.053_6	$7._2$
	3.6	-671.0	226.0	20.8	-4.90	1.089_9	$7._8$
	4.0	-687.0	239.0	22.0	-5.20	1.111_1	$8._3$
	4.6	-681.0	256.0	21.5	-7.07	1.136_7	$8._9$
	5.0	-655.0	267.0	19.3	-8.01	1.147_8	$9._2$
40	0.1	146.0	30.0	-0.054	-0.018	0.931_6	$0._8$
	0.2	155.0	42.3	-0.072	-0.051	0.923_6	$1._2$
	0.3	149.0	51.9	-0.040	-0.093	0.920_6	$1._5$
	0.4	137.0	59.8	0.040	-0.144	0.920_8	$1._7$
	0.5	122.0	66.9	0.165	-0.201	0.922_5	$1._9$
	0.6	106.0	73.3	0.332	-0.264	0.925_2	$2._1$
	0.7	88.9	79.2	0.537	-0.333	0.928_5	$2._2$
	0.8	71.5	84.7	0.776	-0.407	0.932_0	$2._4$
	0.9	54.3	89.8	1.05	-0.485	0.936_7	$2._5$
	1.0	37.2	94.6	1.34	-0.569	0.941_3	$2._7$
	1.2	4.28	104.0	2.00	-0.747	0.951_3	$2._9$
	1.4	-26.5	112.0	2.73	-0.941	0.962_3	$3._2$
	1.6	-54.9	120.0	3.51	-1.15	0.973_9	$3._4$
	1.8	-80.6	127.0	4.30	-1.37	0.986_1	$3._6$
	2.0	-103.0	134.0	5.08	-1.61	0.998_6	$3._8$
	2.6	-155.0	153.0	7.17	-2.38	1.037_4	$4._3$
	3.0	-174.0	164.0	8.11	-2.95	1.063_0	$4._6$
	3.6	-180.0	180.0	8.33	-3.88	1.098_8	$5._1$

TABLE XVI (Continued)

t,°C	m	$\bar{L}_{2H}$	$\Delta\bar{L}_2$	$\bar{L}_{1H}$	$\Delta\bar{L}_1$	Δ_H[b]	$\Delta\phi \times 10^3$
40	4.0	-167.0	189.0	7.39	-4.54	1.112_0	$5._4$
	4.6	-121.0	203.0	3.74	-5.61	1.114_3	$5._7$
	5.0	-71.5	212.0	-0.598	-6.35	1.152_5	$6._0$

[a] Enthalpy data in cal mole^{-1}

[b] From fit of all freezing point data.

APPENDIX III

ENTHALPY DATA FOR OTHER SALTS

TABLE XVII

HEATS[a] OF DILUTION FOR KCL

t, °C	m_i	m_f	ΔH_H^{dil}	ΔH_D^{dil}	$\Delta H_H^{dil} - \Delta H_D^{dil}$
10	3.41	.152	666 ± 1	889 ± 4	-223 ± 4
25			404 ± 9	534 ± 2	-130 ± 10
50			88 ± 9	157 ± 5	-69 ± 10
75			-191 ± 2	-171 ± 2	-20 ± 3

[a] Units are cal $mole^{-1}$

TABLE XVIII

INTEGRAL HEATS OF SOLUTION[a] AND ISOTOPE EFFECTS FOR OTHER SALTS

Salt	t, °C	m	ΔH_H^I	ΔH_D^I	$\Delta H_H^I - \Delta H_D^I$
KCl	10	0.104	4770 ± 26	5614 ± 18	-844 ± 32
	25		4172 ± 69	4721 ± 35	-549 ± 77
	50		3294 ± 21	3699 ± 32	-405 ± 38
	75		2522 ± 9	2842 ± 18	-302 ± 20
NaI	10	0.107	-1270 ± 2	-212 ± 8	-1058 ± 8
	25		-1760 ± 30	-931 ± 25	-829 ± 39
	50		-2372 ± 1	-1722 ± 4	-650 ± 4
	75		-2912 ± 1	-2406 ± 21	-506 ± 21
NaBr	10	0.378	382 ± 5	1250 ± 8	-868 ± 10
	25		-87 ± 4	588 ± 9	-675 ± 10
	50		-707 ± 3	-209 ± 6	-498 ± 7
	75		-1232 ± 16	-865 ± 2	-367 ± 16

[a] Units are cal $mole^{-1}$

VITA

Quentin Douglass Craft was born in Pennington Gap, Virginia on October 12, 1946. He graduated from Pennington High School in June 1965 and then entered Virginia Polytechnic Institute. He received the B.S. degree in chemistry in June 1969. During the summers of 1968 and 1969 he worked in the research laboratories of Tennessee Eastman Company.

He entered graduate school at the University of Tennessee in September 1969 and received the Doctor of Philosophy degree with a major in chemistry in March 1975.